The University of Adelaide

School of Mechanical Engineering

DESIGN, BUILD AND CONTROL OF A SINGLE / DOUBLE ROTATIONAL INVERTED PENDULUM

FINAL REPORT

AUTHORS: Mr. James Driver and Mr. Dylan Thorpe

SUPERVISORS: Dr. Ben Cazzolato and Mr. Rohin Wood

CLIENT: The University of Adelaide

DATE: October 2004

ABSTRACT

Automatic Control is a growing field of study within the School of Mechanical Engineering at Adelaide University. The curriculum covers proportional, integral and derivative (PID), and state space control. PID is widely used in industry and accounts for the vast majority of control systems implemented world wide. To enhance learning, students are given access to several control experiments, designing PID controllers. State control accounts for one third of the automatic control curriculum, but there are no experiments or demonstrations in state controller design.

An inverted pendulum system has been proposed as a suitable State space demonstration and experimentation device. Undergraduate textbooks cover dynamic modelling and state control of single inverted pendulums. Double inverted pendulums, popular amongst the research fraternity, can further demonstrate the intricate control achievable with state space methods. Commercial inverted pendulum experiment rigs are available but are cost prohibitive.

This report begins with an outline of the research into inverted pendulum system design and control along with mathematical modelling methods. Details of the pendulum as a mechatronic system are presented and mathematical modelling of the designed system follows. Controller design and implimentation is discussed next. Results from testing the pendulum are presented in section 8. The report concludes after a discussion of the project exhibition and brief financial analysis.

ACKNOWLEDGEMENTS

The Authors of this report would like to thank all of those involved in this project. These people are;

Supervisors,

Dr. Ben Cazzolato

Mr. Rohin Wood

Workshop Staff,

Mr. Joel Walker

Mr. Silvio De leso

Mr. George Osborne

Mr. Derek Franklin

Mr. Ron Jager

Mr. Bill Finch

Proof Readers,

Ms. Sue Thorpe (Mum)

Ms. Julia Hinsliff

TABLE OF CONTENTS

List of Figures

List of Tables

Notation

The notation throughout the following text adheres to the following conventions

The state variables of link 1 will be:

θ_1 : Angle of link 1 in the horizontal plane

$\dot{\theta}_1$: Angular velocity of link 1 in the horizontal plane

$\ddot{\theta}_1$: Angular acceleration of link 1

The state variables of link 2 will be:

θ_2 : Angle of link 2 in the vertical plane

$\dot{\theta}_2$: Angular velocity of link 2 in the vertical plane

$\ddot{\theta}_2$: Angular acceleration of link 2

The state variables of link 3 will be:

θ_3 : Angle of link 3 in the vertical plane

$\dot{\theta}_3$: Angular velocity of link 3 in the vertical plane

$\ddot{\theta}_3$: Angular acceleration of link 3

J_1: The moment of inertia of link 1 about its centre of mass

J_2: The moment of inertia of link 2 about its centre of mass

J_3: The moment of inertia of link 3 about its centre of mass

l_2: The distance from the centre of rotation of link 2 to the centre of mass

l_3: The distance from the centre of rotation of link 3 to the centre of mass

m_1: The mass of link 1

m_2:The mass of link 2

m_3:The mass of link 3

g: is gravity (g=9.81 m/s^2)

L_1 : Length of link 1

L_2 : Length of link 2

L_3 : Length of link 3

b_1: is the viscous damping coefficient of the bearing on which the link 1 rotates

b_2: is the viscous damping coefficient of the bearing on which the link 2 rotates

b_3: is the viscous damping coefficient of the bearing on which the link 3 rotates

K: is kinetic energy

P: is potential energy

L: is the Lagrangian

1. INTRODUCTION

Inverted pendulum systems make good bench top demonstrations of automatic control techniques. They are nonlinear, unstable systems which showcase modern control methods and have the added bonus of being exciting to watch. Balancing a broom in one's hand is an example of an inverted pendulum and is often demonstrated in classrooms. It gives a good physical system to observe and understand (drawing free body diagrams, seeing where the hand moves to keep the broom stable), but there is no test rig within the University of Adelaide's School of Mechanical Engineering which allows students to experiment quantitatively with the control of an inverted pendulum. This broomstick example is a two-degree-of-freedom single inverted pendulum. By restricting consideration to only one degree of freedom gives the classic textbook example of a nonlinear unstable system. Using modern control techniques, it is possible to control multi-degree-of-freedom or multiple pendulum systems.

1.1 Project Definition

The project definition was written at the beginning of the project and contains all that the authors hoped to achieve. It is included here verbatim so that the project results can be put in context.

The project "Double Inverted Pendulum" aims to design, build and control a double inverted pendulum. While balancing two links end on end seems impossible, computer control gives us the ability to balance two or more links. The whole system should be small enough to be portable for use on and off campus as a demonstration in classrooms and departmental exhibits. Physically the plant should be rugged enough to allow people to attempt balancing the pendulum manually to give them a better idea of the degree of difficulty involved in the control method. This double inverted pendulum system could be extended to have more links, so some degree of modular design should be utilised.

Additionally, a swing up controller will be investigated. Swinging the pendulum up from stable equilibrium allows the system to work without manual setup, increasing the enjoyment for an audience and adds an extra amount of complexity for the designers. If time permits, there are two more investigations that could yield interesting results; Linear

Quadratic Regulator (LQR) optimal control compared with sliding control, and the use of estimators in the state model. Sliding control claims to increase the angle from vertical over which an inverted pendulum can be controlled. Estimating a state would reduce the cost and complexity of the system by removing a transducer, or allow more vertical links to be added without extra hardware overheads.

The project will begin with a review of available literature about inverted pendulum systems. Some components, in particular the motor and encoders will be generic for any system design. These will be selected and obtained as early as possible to allow modelling in Computer Aided Design (CAD) software. Mathematical models will be developed, first for a single inverted pendulum, as the necessary equations of dynamic behaviour for the single inverted pendulum are readily available from textbooks. A comparable set of equations for the double pendulum will be derived. Concurrent work will go into the physical design of the system, to determine desirable geometry for control and aesthetics. The electrical system should be designed for high sample rate and neat presentation.

2. LITERATURE REVIEW

2.1 Introduction

The literature review undertaken as a part of the double inverted pendulum project was focussed on understanding the background and application of inverted pendulum systems, mathematical modelling, control, mechanical design aspects and other successful projects of a similar nature.

2.2 Background

The inverted pendulum is a classic example of a non-linear control topic and one studied frequently with reference to design, implementation and development of control for non-linear systems. It appears in undergraduate control text books such as Dorf and Bishop (1998) where it is used as an example of how to mathematically describe physical systems.

2.3 Present Applications

Inverted pendula are currently used as teaching aids and research experiments. Quanser (2004), a supplier of educational and research based equipment produce modular systems which can be configured as single or double inverted pendula. Their range offers both a rotary and a linear version. Many researchers have also built their own inverted pendulum systems (Åström and Furuta, 1996; Brockett & Hongyi, 2003; Rubi, 2002) to suit their investigations.

2.4 System Modelling Methodology

Zhong and Röck (2001) indicate that the system of dynamic equations describing a double inverted can be derived by Newtonian methods (using free body diagrams) or the Euler-Lagrange (or just Lagrange) method. The Euler-Lagrange method derives the system equations by applying the Euler-Lagrange equation to the Lagrangian. The Lagrangian is defined as the difference between potential and kinetic energy ($L=K-P$). The Lagrange method simplifies the mathematical derivation substantially. The

California Institute of Technology, (1994) give a treatment of the Lagrange approach, which is the preferred method throughout the literature reviewed for this project.

When implementing control in the real world system identification needs to take place. Zander, (2002) outlines methodologies for determining mechanical damping properties of linear systems which can be applied to the pendulum system. Wolfman (2004) describes modelling of constant field DC motors. This information was used in implementing the controller designs on the real test rig. Determining the centre of mass and moment of inertia of each of the modelled links was done using the design drawings, component data, and the parallel axis theorem as outlined in Efunda (2004).

In modeling real world systems, attention needs to be paid to measurement noise. Katupitiya and Luong (circa 2001) outline methods of Kalman filtering specifically designed for deriving velocity measurement from encoder readings. This should be reviewed by future workers.

2.5 Inverted Pendulum Configurations

The literature covers a variety of inverted pendulum designs. The system configuration depends on two factors, the method of actuation and the number of degrees of freedom. There were two types of actuation reviewed, linear and rotary. The actuation methods are discussed in section 2.5.1.

The simplest controllable inverted pendulum would consist of a pendulum link directly coupled to a motor shaft (Dorf and Bishop, 1998). This configuration could be controlled open-loop with the use of a stepper motor, however, it is deemed too simple for further consideration. Therefore the simplest controllable inverted pendulum system that shall be considered must have at least two degrees of freedom, one for the position of the base of the pendulum and the other for the pendulum angle. For two degrees of freedom, the base of the pendulum is restricted to only moving in one dimension (linear or rotary) and the pendulum angle can vary only in one dimension. For a higher degrees of freedom, either more single degree of freedom links are added, or the existing links are allowed to move in multiple dimensions.

2.5.1 Two Degree of Freedom Configurations

In the linear case, a motor is used to move a cart along a straight track as shown in Figure 2.1. The pendulum is attached to the cart by a pin joint. The axis of rotation of the pendulum link about the pin joint is horizontal and perpendicular to the cart's direction of travel. The input to the system is the force applied to the cart, via the motor. Full derivations of the system dynamics for a linear inverted pendulum can be found in Dorf and Bishop (1998) and Franklin (2002). A reproduction of the diagram is shown in Figure 2.1 where F is the input force, x is the linear displacement and θ is the angular displacement of the pendulum link.

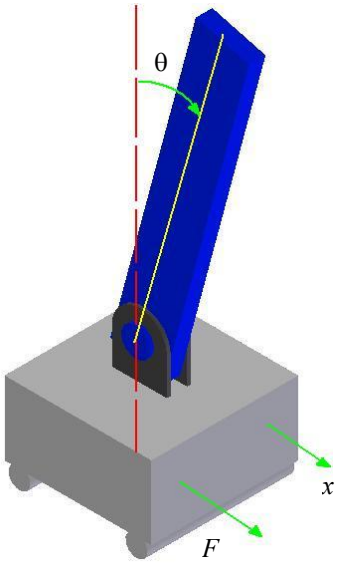

Figure 2.1 A linear single inverted pendulum

For the rotary configuration, as seen in Figure 2.2, the base of the pendulum is attached to a horizontal link via a pin joint. The axis of revolution of the pendulum is collinear with the long axis of the horizontal link. The angle of the pendulum link is θ_2. The horizontal link is coupled either directly or via gearing to the motor shaft giving it rotary motion (Quanser, 1996). The angular position of the rotary link is θ_1. The input to the system is the torque T, applied by the motor.

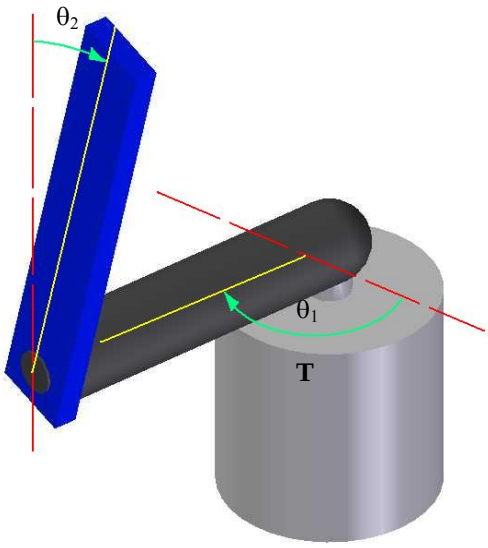

Figure 2.2 A rotary single inverted pendulum

2.5.2 Multiple Degree of Freedom Configurations

Theoretically, any number of links can be mounted on the cart or rotor and successfully held in the all-up configuration (Cazzolato, 2004a). The most reported to have been successfully balanced is four (Googol, 2004). Video footage of this feat can be viewed at the Googol website. Three link systems (triple inverted linear pendulum) have been observed as demonstrated by the Max Plank Institute (2004) and Quanser (2004). For all of these systems, each link (including the rotary link or cart) has only one degree of freedom. Figure 2.3 (a,b) show rotary and linear versions of double inverted pendula. In Figure 2.3a, T is the input torque, θ_1 is the angular position of the horizontal link, θ_2 is the angular position of the first pendulum link and θ_3 is the angular position of the second pendulum link. In Figure 2.3b, F is the input force, x is the position of the cart, θ_1 is the angular position of the first pendulum link and θ_2 is the angular position of the second pendulum link. For triple or quadruple configurations, more pendulum links are added in a similar fashion, end to end.

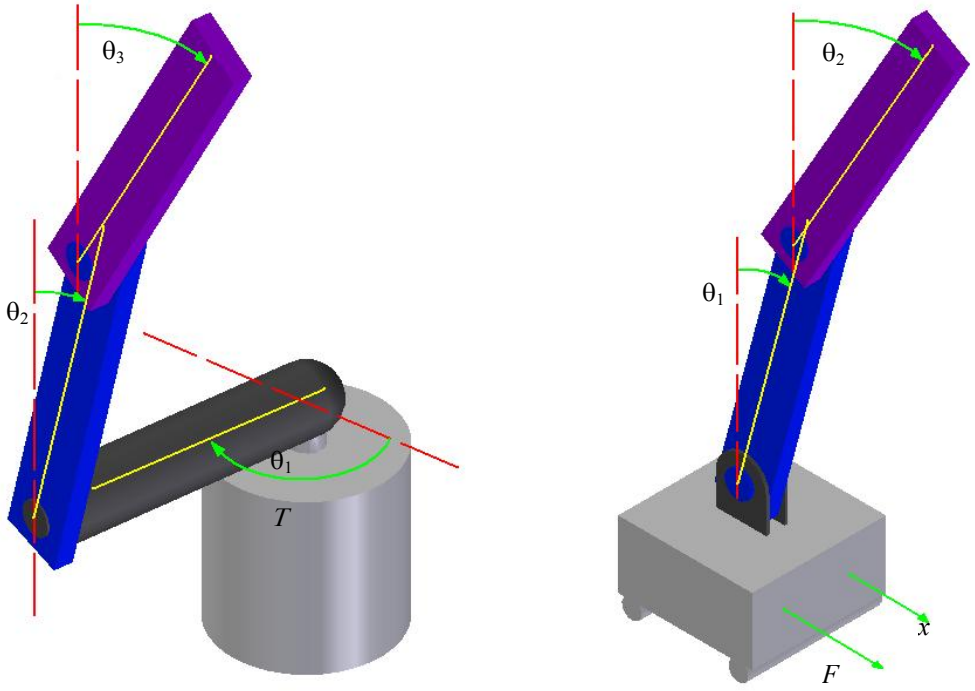

Figure 2.3 (a) A rotary double inverted pendulum, (b) A linear double inverted pendulum

Viewing diagrams and video footage of multiple link systems, it is apparent that the bottom links (closest to the cart or rotary link) are made shorter than the upper links.

The additional links do not have to be configured end to end as in figure 2.3. The cart or rotational link can have multiple links attached directly. This is shown in figure 2.4 for (a) the rotational case, and (b) the linear case. Labelling of system parameters is the same as in figure 2.3. These arrangements can be considered parallel double inverted pendula, while those shown in Figure 2.3 are in serial arrangement (Googol Technology, 2004(2/8/04))

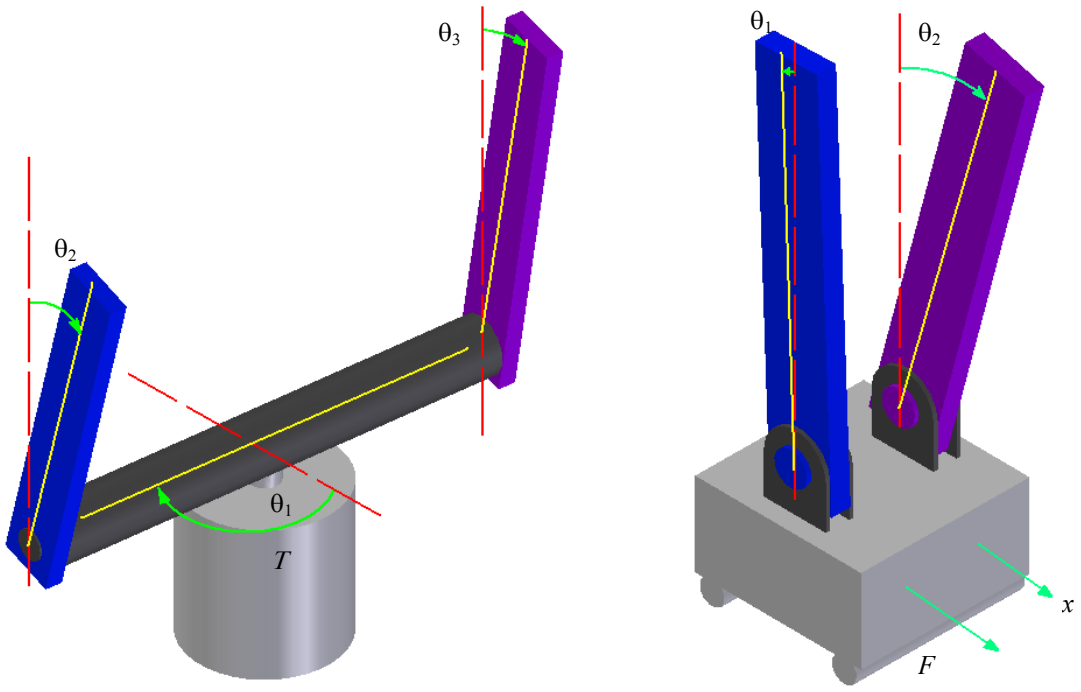

Figure 2.4 Parallel arrangement of double inverted pendula (a) rotary and (b) linear

Googol Technology Ltd. produces a rotational pendulum experimentation rig which allows the double parallel pendulum arrangement shown in figure 2.4(a). The Googol rotational rig allows for serial-parallel configuration where one of the two single pendula is replaced by a double pendulum. The linear case (figure 2.3(b)) is produced by Quanser (2004).

As mentioned in section 2.5, a pendulum link can be allowed to move about two axes instead of one axis. The base point of the pendulum link must then be actuated in two degrees of freedom, which form a horizontal plane. These systems are called planar inverted pendula (Googol Technology, 2004). Planar inverted pendula can be implemented with pure rotary, pure linear or a combination of rotary and linear actuation. These configurations are shown in figure 2.5.

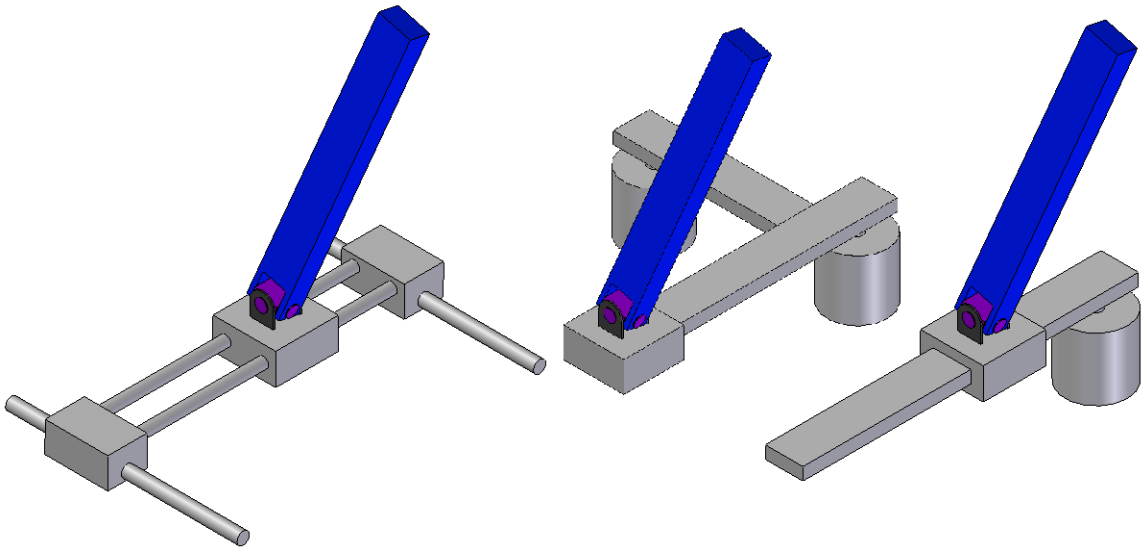

Figure 2.5 Planar single pendulum in (a) linear-linear; (b) rotary-rotary and (c) rotary-linear configuration

The linear, linear case of figure 2.5(a) is featured in the virtual reality toolbox for MATLAB. There is a demonstration program (`vrpend.mdl`), included as a part of the virtual reality toolbox in Matlab, which simulates a two degree of freedom single inverted pendulum. A screen shot from the simulation is shown in Figure 2.6 (Mathworks, 2004).

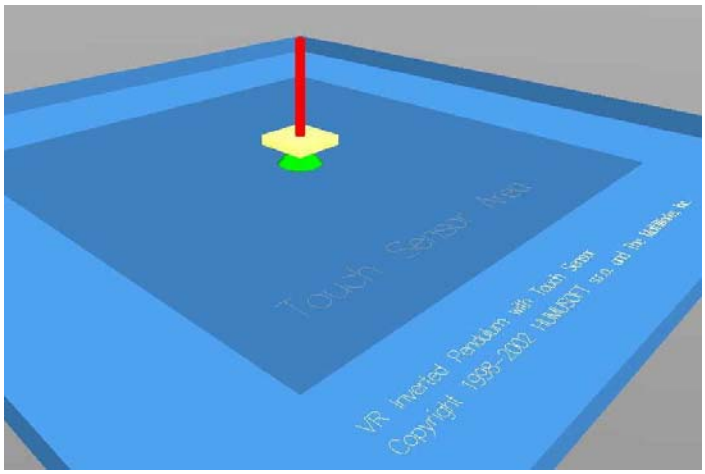

Figure 2.6 Two degree of freedom virtual single inverted pendulum from Matlab

Balancing a broomstick in one's hand is cited in textbooks (Dorf and Bishop, 1998) and demonstrated in lecture courses (Cazzolato, 2004b). This is another example of the two degree of freedom single inverted pendulum. Considering the shoulder and elbow as revolute joints, this is best represented by figure 2.5(b), a rotary, rotary configuration.

Googol Technology produces both linear-linear and rotary-rotary planar inverted pendulum devices.

Planar inverted pendula can also be configured with multiple pendulum links. Googol Technology Ltd produces a unit which has three serial links over a linear or rotational planar actuation system. Video footage of this device can be viewed at their web site (Googol Technology, 2004)

2.7 Control Methodology

Some of the literature considers swinging the pendula from the stable position (all links down) to the 'all up' position using the motor input torque. This is called swing-up control. Some of the literature only considers controlling the system once it is already in the upright position. One could assume that in these cases, the pendulum link(s) are held upright and stationary by the experimenters while the controller is initialised.

In many cases that consider only swing-up or swing-up and stationary control, it is accepted that two different control algorithms are required, and that there needs to be a switch between the controllers affected in software at a time when the inverted pendulum can be controlled by the stationary controller. This occurs for the single pendulum when θ_2 and $\dot{\theta}_2$ are within the domain of attraction (the range for which the stabilisation controller will function satisfactorily) and for the double pendulum when θ_2, θ_3 and $\dot{\theta}_2, \dot{\theta}_3$ are within the domain of attraction. Each controller, swing-up or stationary control is considered independently of the other.

2.7.1 Stabilisation of Unstable Equilibriums

In the following methods the second order coupled nonlinear equations were linearised about the equilibrium of interest in order to fit them to the linear scheme of state space control. Linearising the equations of motion was done generally in Wolfram Research (2004) using Taylor series or by making assumptions of small angles and small velocities.

The California Institute of Technology (1994) describe the use of pole placement in a full state feedback controller. The document is an experiment instruction handout, and part of the experiment is to use different gains to see how they affect the system's response. There is no discussion on how to find the optimal gain matrix.

Zhong and Rock (2001) used a linear quadratic regulator (LQR) to optimise the control gains used in the feedback controller. The LQR optimises a performance function which trades off setpoint following with control effort by solving the Ricatti equation for the given system and weighting matrix.

Utkin et al. (1999) suggest that sliding mode control offers a greater domain of attraction for the linearised model stabilisation of the unstable upright equilibrium. Essentially sliding mode control is a method of control by which a non linear (discontinuous) control effort is chosen in such a manner as to enforce sliding modes, or in other words linear behaviour along some sliding mode of attraction. This is a form of control that may be investigated further depending on the time constraints of the project.

2.7.2 Swing-up Control

Two approaches to swing-up control have been reviewed. Zhong and Rock (2001) describe an energy shaping approach. The cart is accelerated such that the amount of kinetic energy in the system is equal to the amount of potential energy stored by both links being balanced upright. When the direction of the cart's motion is suddenly reversed, there is enough kinetic energy and momentum in the pendulum links for them to swing into the upright position. The controller is developed using partial feedback linearisation and passivity based control.

Rubi (2002) uses a trajectory following strategy. First, he assumes that all links are actuated, and as such the pendulum links can be moved from hanging to inverted along any valid trajectory. A trajectory is considered valid if the pendulum starts and finishes with zero velocity. The optimum trajectory is calculated to reduce the torques at the pendulum links as close to zero as possible. Other factors such as rise time and track length are included in the optimisation problem, but the two pendulum torques have the heaviest cost weighting applied in solving the optimal trajectory problem. The residual

torques are then considered as disturbance inputs to the under-actuated system, and a feedback controller is designed to increase disturbance rejection.

For the single inverted pendulum a simple bang-bang method as described by Åström and Furuta (1996) can be applied. This method regulates energy content in the system. Energy is added to the system with a stepped signal until the desired energy level is achieved.

Other methods of swing-up control are outlined in Kobayashi et al. (circa 2001) and Komine et al. (circa 2000) and should be reviewed by future workers.

3. MECHATRONIC DESIGN

The double inverted pendulum system has been designed with the two pendulum links stacked end on end, in a serial configuration. Actuation is rotary, via a direct attachment of the horizontal link to the motor shaft. Section 3 discusses the system that has been developed. The mechanical system, consisting of the pendulum and driven links, and the support structure were required to fulfil the following requirements:

- The pendulum rig should be easily transported
- The rig should be a stand alone desk top presentation device
- The rig should be structurally robust and free from stiction (static friction), backlash and out of plane slackness
- System dynamics should be slow enough to allow controllability
- There should be provision for attempts at manual control
- The rig must fit the following aesthetic criteria:

  - must look like a professional/ commercial quality product

  - must look "engineering"
- The rig should be designed to have a satisfactory life

The electronic system, which is made up of the sensors, actuator and signal processing equipment needed to fulfil the following requirements:

- Perform with a high degree of accuracy
- Allow high rate of data acquisition
- All wiring and hardware to be housed internally for improved aesthetics

3.1 Design Parameters

Consideration of the preceding design requirements resulted in the formulation of the following design parameters:

- To be a desktop application and easily transported, the device should not be taller than about one metre in the off position, which will result in an upright height of less than two metres. Further the device should not be so heavy as to require

lifting machines or special transportation requirements, in other words it should be light enough to lift into the back of a car.

- To be structurally robust, the base of the system must be heavy enough to stop momentum in the pendulum links toppling the system.
- To make the dynamics of the system slow it is required to make the vertical links as long as possible noting that the middle link must be a little faster (physically shorter) than the terminal link.
- For the rig to be free of stiction, backlash and out of plane movement the rig should be constructed of quality components and the use of gears avoided.
- The remaining constraints can be satisfied by mechanical design of chassis and panelling.

3.2 Mechanical Design

The structural requirements for the pendulum rig were that it be stiff enough to avoid un-modelled poles and of a reasonable size for transportation, demonstration and control. With this in mind it was decided that the pendulum links should be at about 400mm in length and the driven link at about 200mm in length.

The supporting structure is essentially a column fixed to a plate which forms the base. The column is a tube with a large enough diameter to house the motor and electronics hardware. The column is taller than the combined height of the pendulum links to ensure these links will not hit the base plate if hanging or swinging in the down-down position. The base is big enough to provide a low centre of mass, which helps avoid toppling of the structure, and has a suitable diameter to give a well balanced, pleasing appearance.

The pendulum system consists of three links. The horizontal link (link 1) is coupled directly to the input motor at one end, and holds a shaft encoder at the other end. The shaft of this encoder supports the base of the first pendulum link (link 2). Another encoder is housed at the end of link 2 which supports the second pendulum link (link 3). Figure 3.1 shows a cutaway view of the double pendulum assembly.

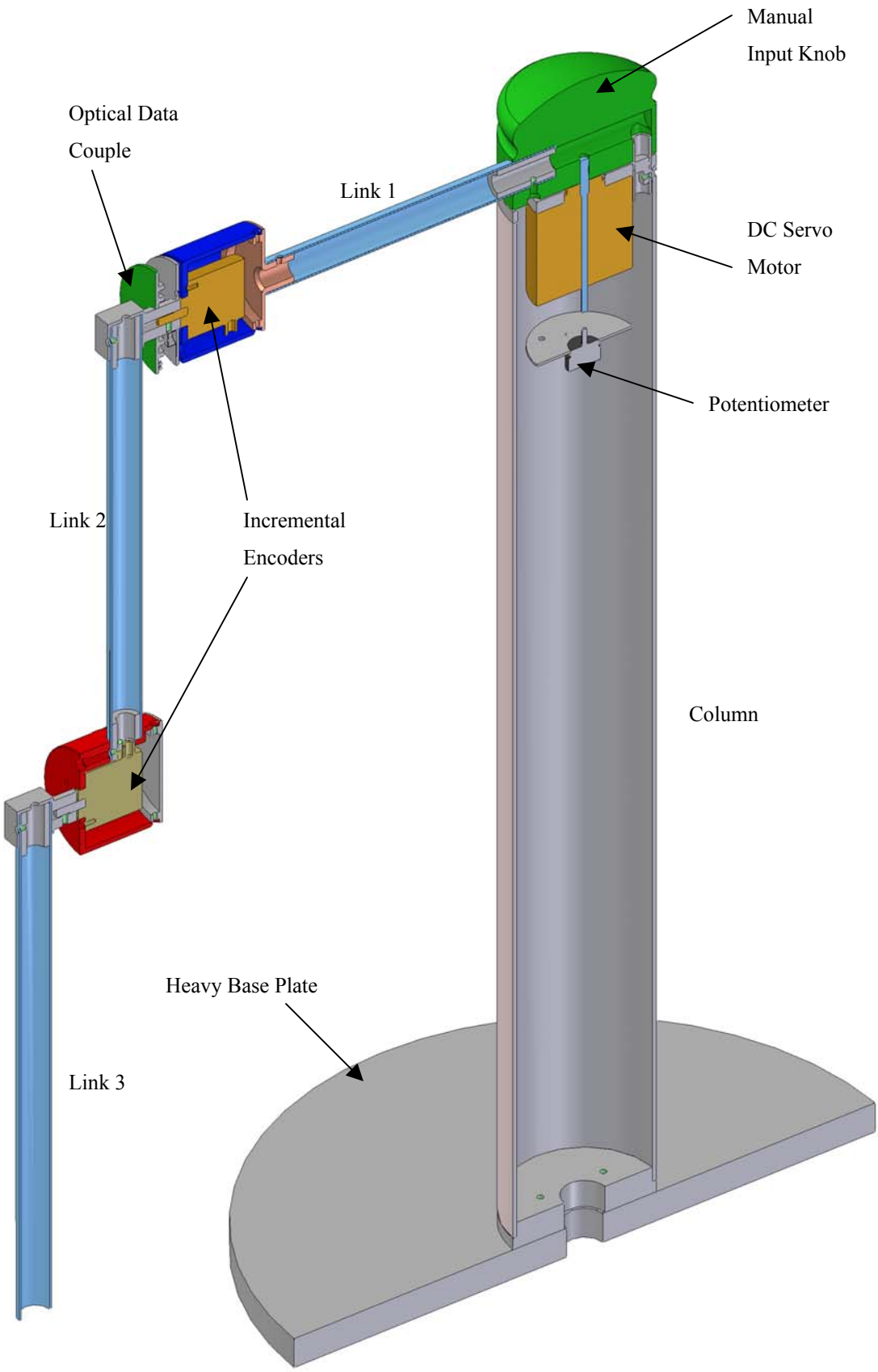
Manual
Input Knob
Optical Data
Couple
Link 1
DC Servo
Motor
Potentiometer
Link 2
Incremental
Encoders
Column
Heavy Base Plate
Link 3

Figure 3.1 Cutaway view of double inverted pendulum plant

The encoders are housed in cylinders and all wiring runs through the links to achieve the desired clean looks.

3.3 Electronic Design

The electronic design of the double inverted pendulum is concerned with selecting the actuator, sensors, controller and providing a reliable data transmission route.

The actuator is a RS brand low inertia DC servo motor. Figure 3.2 shows a photograph of the motor (RS Components, 2004).

Figure 3.2 The DC servo motor from RS

Table 3.1 shows the motor's specifications.

Table 3.1 Specification of DC servo motor

Maximum Continuous Torque	12 N·cm
Maximum Peak Torque	27 N·cm
Motor Voltage Constant	10.3 V/1000rpm
Motor Torque Constant	9 N·cm/A
Mechanical Time Constant	17 ms

Rotor Inertia	0.214 $kg \cdot cm^2$
Rotor Resistance	7.8 Ω
Rotor Inductance	5.0 mH

Three sensors are needed in the double inverted pendulum, one for the position of each link. The driven link's rotational position is measured by a precision potentiometer coupled to the motor's second shaft. Figure 3.3 shows the potentiometer (RS Components, 2004).

Figure 3.3 Servo-mount precision potentiometer

The potentiometer is used here because the control interface only has two encoder inputs and these are used for the pendulum link sensors. The potentiometer is suitably linear, with a rated error of 0.2% in linearity.

The encoders chosen for the pendulum links' state feedback are Omron incremental shaft encoders Figure 3.4 (RS Components, 2004). Incremental encoders generate a square wave signal in response to shaft rotation. By using two such pulse waves, direction of rotation is also determined, see Figure 3.5 (RS Components, 2004).

Figure 3.4 Omron optical encoder

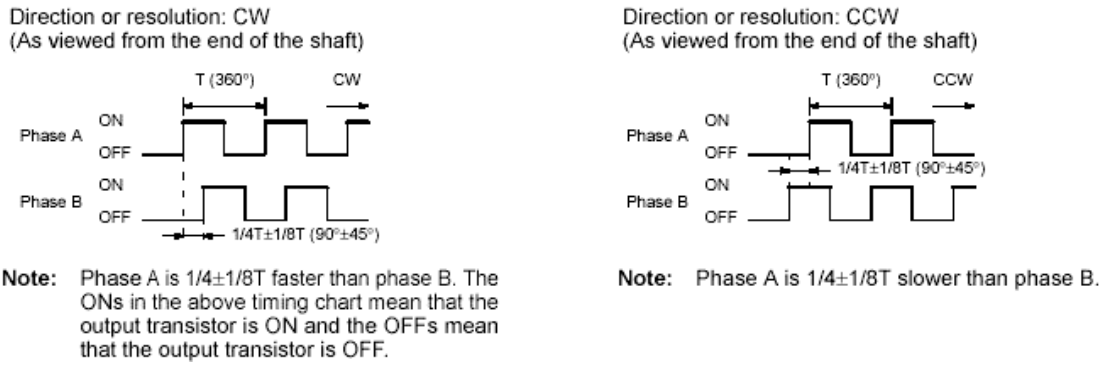

Figure 3.5 Encoder output signal

The encoder selected produces 1000 pulses per revolution, and the software, Simulink reads this signal in quadrature. A quadrature signal uses the phase difference between the two pulse waves to estimate the encoder's position between pulsing positions. A signal produced at 1000 pulses per revolution in quadrature will produce 4000 reference points per revolution, 1000 major points based on one pulse wave and another 3000 reference points inferred from the phase difference of two pulse signals.

A personal computer incorporating a DSpace-1102 interface card is used as the controller hardware. In the future, both of these could be replaced by a micro-controller.

Each vertical link must be able to rotate any angle or even whole revolutions about its joint. Having a cable running from the encoder at the end of the first pendulum link (link 2) to the system base would hinder this free motion and reduce the aesthetic appeal of the system. Three possible solutions for this problem have been formulated: firstly, the middle link could contain a power source and wireless data transmitter to communicate with the base. This concept has a few drawbacks: batteries and a transmitter would be difficult to conceal in a professional looking design. Small batteries would have a limited time of charge. If the system was on display, it would have to be recharged periodically. Transmitting the second encoder's position by radio frequency would induce a time delay into the system. This is very undesirable, as it makes control difficult and less robust.

The second concept is to use sliprings to transmit power to the encoder and data back to the controller. Sliprings create considerable amounts of noise in the electrical signals and increase the amount of friction in the joint. Small sliprings (to enhance aesthetics) would need to be sourced from a specialist manufacturer and could be quite expensive.

The third concept is to create an optical data couple. The signal out of the encoder can be used to drive a series of light emitting diodes (LEDs) on a printed circuit board (PCB) attached to the base of link 2. These LEDs could trigger a light sensor on a PCB that is attached to the end of link 1 and facing the first PCB. With enough LEDs and/or a diffusing lens, a solid ring of light could be made. This ring of light would enable the light sensors to reproduce the pulses of the encoder output regardless of link 2's position or velocity. Power could be supplied to the encoders by a slipring style system, using brushes from a small DC motor on one board and tracks etched into the other PCB.

It was decided to investigate the design of option 3, the optical data couple further. CAD models of each circuit board have been produced, and are shown in Figures 3.6 and 3.7.

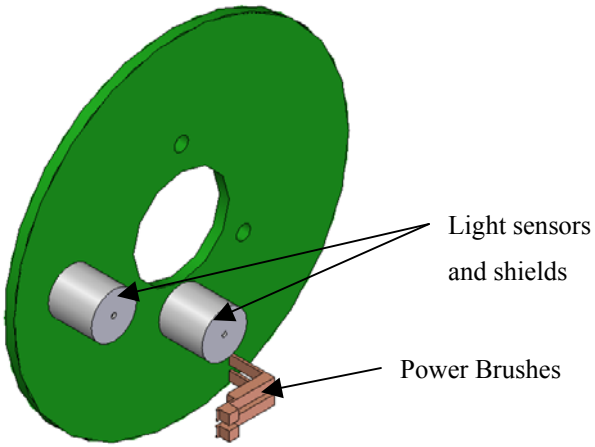

Figure 3.6 Data receiver side of the optocouple link

The encoder has two outputs which enables a software driver to determine the direction of rotation. Using an optical coupling for the data transmission requires that each sensor only receives one signal. Shielding from crosstalk must be included in the design. The two cylinders protruding from the PCB in Figure 3.6 reduce each light sensor's range of vision, such that cross talk is eliminated. Other options for channel separation included spacing the sensors further apart, or using different colour LEDs for each channel and using an optical filter, like cellophane on the receivers. The two conductors closest to the edge of the circuit board are connected to the power supply.

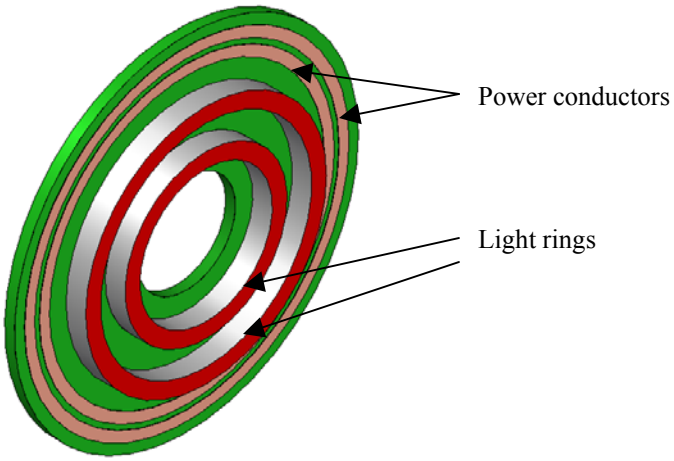

Figure 3.7 Data transmitter side of the optocouple link

The red rings in Figure 3.7 are diffusing rings. Each ring is illuminated by eight surface mount LEDs. They are set at the same radii as the sensors on the other board. The two copper tracks touch the protruding conductors on the other board when mounted and form the power supply rails for the encoder.

Testing of the data couple has shown that with a regulated power supply, data can successfully be transferred at up to 2 kilohertz. This corresponds to a shaft rotational velocity of 120 revolutions per minute or 12.4 radians per second. In place on the pendulum rig, fluctuations in supply voltage produce false flashing of the LEDs. This makes the output signal unusable for control of the system, configured as a double inverted pendulum.

4. MATHEMATICAL MODELS

4.1 Introduction

When approaching the solution of a control problem, mathematical modelling is the basis of many of modern control strategies.

The more that is known about a dynamic system, the more accurate a mathematical model can be. Accurate mathematical modelling allows the design of faster, more accurate and effective controllers. This is because mathematical models allow design, test and development of controllers rapidly using Matlab even before the physical rig is constructed.

Accurate mathematical models of the pendulum system can be developed provided that there is not excessive stiction (static friction), backlash or bearing slack present. The fore mentioned non linearity's make accurate modelling and control of the system much more difficult.

4.2 Mathematical Modelling

Figure 4.1 shows the basic configuration of the double inverted pendulum system that was modelled.

The arrows on the arcs denote the positive direction for the state variables of the plant. The straight vertical lines denote the zero data of the displacement states.

For example when the horizontal link is centered and the vertical links in the downward position, all of the position variables are zero.

The state variables of link 1 are:

θ_1 : Angle of link 1 in the horizontal plane

$\dot{\theta}_1$: Velocity of link 1 in the horizontal plane

$\ddot{\theta}_1$: Acceleration of link 1

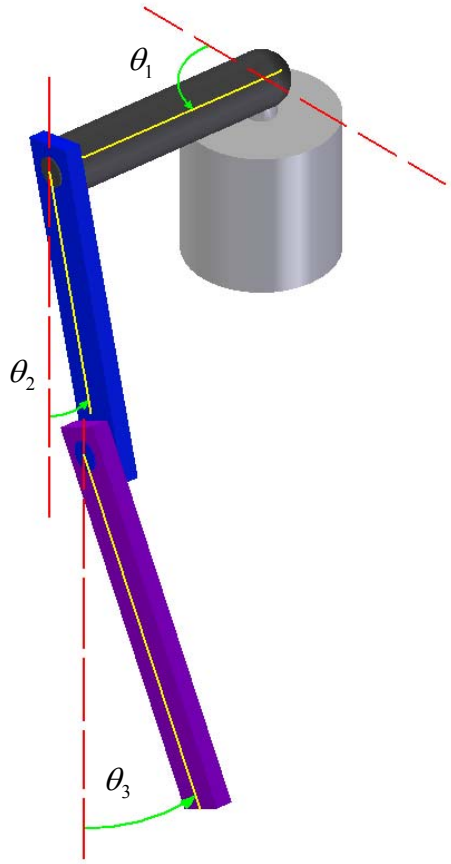

Figure 4.1 Schematic of double inverted pendulum

The state variables of link 2 are:

θ_2: Angle of link 2 in the vertical plane

$\dot{\theta}_2$: Velocity of link 2 in the vertical plane

$\ddot{\theta}_2$: Acceleration of link 2

The state variables of link 3 are:

θ_3: Angle of link 3 in the vertical plane

$\dot{\theta}_3$: Velocity of link 3 in the vertical plane

$\ddot{\theta}_3$: Acceleration of link 3

J_1, J_2 and J_3 represent the moments of inertia of the respective links about their centre of mass, l_2 and l_3 are the distance from the centre of rotation of the link to the centre of mass of the respective links, and m_1, m_2 and m_3 are the masses of links 1, 2 and 3 respectively. The symbol **g** is gravity and is **g**=9.81 m/s^2 towards the centre of the earth. L_1, L_2, L_3, are the lengths of links 1, 2, and 3. The variables b_1, b_2, and b_3 are the viscous damping coefficients of the bearings on which the links rotate.

To derive the equations of motion of the single inverted pendulum system the free body diagrams of the system subcomponents were considered. For the single inverted pendulum system the Newtonian approach of applying Newton's laws of motion was used to derive the governing differential equations. The previously mentioned approach becomes highly complicated for the double inverted pendulum and hence the Euler Lagrange method was applied in the derivation of the equations of motion for the double inverted pendulum dynamics.

4.2.1 Mathematical Model of the Single Inverted Pendulum

First the model of the single inverted pendulum was considered using the above definitions and considering the 3rd link as an extension of the 2nd. First consider the free body diagram of the horizontal (driven) link. (Figure 4.2)

Sum the moments about the centre of rotation,

$$M = J\ddot{\theta}$$

$$J_1\ddot{\theta}_1 = \tau - \mathrm{n}L_1 - b_1\dot{\theta}_1 \qquad \textit{Equation } 4.1$$

Where variables are defined as follows:

M: Moment positive anti clockwise.

J: Moment of inertia.

J_i: Moment of inertia of link i.

$\ddot{\theta}$: Angular acceleration.

$\ddot{\theta}_i$: Angular acceleration of link i.

$\dot{\theta}_i$: Angular velocity of link i.

θ_i: Angular displacement of link i.

b_i: Viscous damping of pivot for link i.

n: Force as shown in Figure 4.2.

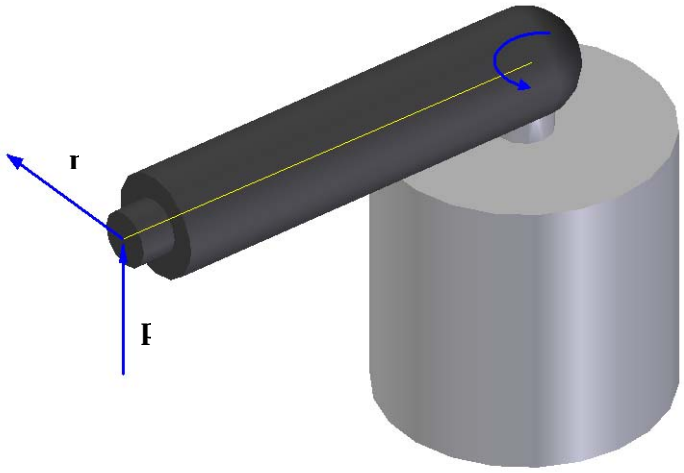

Figure 4.2 Free body diagram of horizontal link

Now consider the free body diagram of the pendulum link (un-driven). (Figure4.3)

Summing forces in the horizontal direction we get,

$$F = ma$$

$$\begin{aligned} \mathrm{n} &= L_1\ddot{\theta}_1 m_2 + m_2 l_2 \ddot{\theta}_2 \cos\theta_2 \\ &\quad - m_2 l_2 \dot{\theta}_2^2 \sin\theta_2 \end{aligned} \qquad \textit{Equation } 4.2$$

Where variables are defined as follows:

F: Force.

n: Force as shown in Figure 4.2.

p: Force as shown in Figure 4.2.

m: Mass.

m_i: Mass of link i.

a: Acceleration.

L_i: The length of link i.

l_i: The length from the center of rotation of link i to its center of mass.

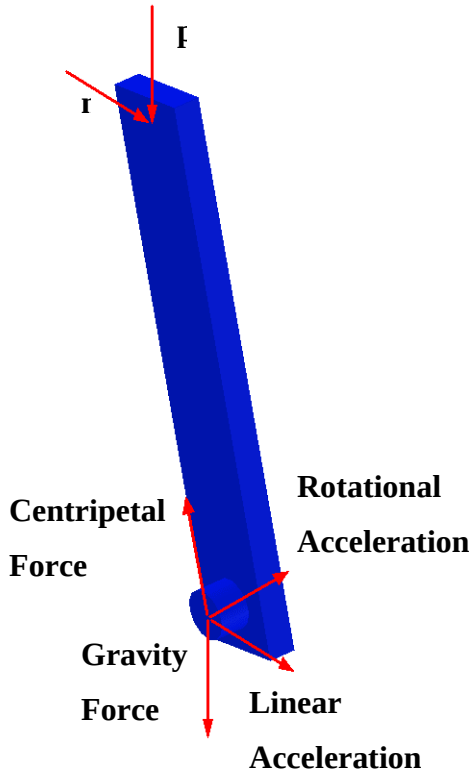

Figure 4.3 Free body diagram of pendulum link

Now if forces are summed perpendicular to the pendulum link the result is,

$$\mathrm{n}\cos\theta_2 - \mathrm{p}\sin\theta_2 - m_2 \mathrm{g}\sin\theta_2 = m_2 l_2 \ddot{\theta}_2 + m_2 L_1 \ddot{\theta}_1 \cos\theta_2 \qquad \textit{Equation } 4.3$$

Summing moments about the pendulum centre of mass yields,

$$J_2 \ddot{\theta}_2 = \mathrm{p} l_2 \sin\theta_2 - \mathrm{n} l_2 \cos\theta_2 - b_2 \dot{\theta}_2 \qquad \textit{Equation } 4.4$$

If Equation 4.3 is multiplied by l_2 and the result added to Equation 4.4, the result is,

$$(\mathrm{n}\cos\theta_2 - \mathrm{p}\sin\theta_2 - m_2 \mathrm{g}\sin\theta_2 = m_2 l_2 \ddot{\theta}_2 + m_2 L_1 \ddot{\theta}_1 \cos\theta_2) \times l_2$$
$$+ (\mathrm{p} l_2 \sin\theta_2 - \mathrm{n} l_2 \cos\theta_2 - b_2 \dot{\theta}_2 = J_2 \ddot{\theta}_2)$$
$$= (-m_2 l_2 \mathrm{g}\sin\theta_2 - b_2 \dot{\theta}_2 = m_2 l_2^2 \ddot{\theta}_2 + m_2 l_2 L_1 \ddot{\theta}_1 \cos\theta_2 + J_2 \ddot{\theta}_2)$$

This can be simplified to

$$\ddot{\theta}_2 (m_2 l_2^2 + J_2) = -m_2 l_2 \mathrm{g}\sin\theta_2 - b_2 \dot{\theta}_2 - m_2 l_2 L_1 \ddot{\theta}_1 \cos\theta_2 \qquad \textit{Equation } 4.5$$

If Equation 4.2 is substituted into Equation 4.1 the result is,

$$J_1\ddot{\theta}_1 = \tau - (L_1\ddot{\theta}_1 m_2 + m_2 l_2 \ddot{\theta}_2 \cos\theta_2 - m_2 l_2 \dot{\theta}_2^2 \sin\theta_2)L_1 - b_1\dot{\theta}_1$$

which simplifies to

$$\ddot{\theta}_1(J_1 + L_1^2 m_2) = \tau - m_2 l_2 L_1(\ddot{\theta}_2 \cos\theta_2 - \dot{\theta}_2^2 \sin\theta_2) - b_1\dot{\theta}_1 \qquad \textit{Equation } 4.6$$

Equations 4.5 and 4.6 are the coupled non-linear equations for the single rotary pendulum system.

4.2.2 Mathematical Model of the Double Inverted Pendulum

The derivation of the mathematical equations describing the dynamics for the double rotary pendulum system took a different approach to the single rotary pendulum. The Euler Lagrange approach was used due to significant mathematical simplifications.

The Lagrangian is defined as the difference between Kinetic and Potential Energy and is used with the Euler Lagrange equation as follows.

$$L = K - P \qquad \textit{The Lagrangian} \qquad \textit{Equation } 4.7$$

$$\frac{d}{dt}\left(\frac{\partial L}{\partial \dot{q}}\right) - \frac{\partial L}{\partial q} = Q_q \qquad \textit{The Euler Lagrange Equation,} \qquad \textit{Equation } 4.8$$

Where,

K is the kinetic energy of the system.

P is the potential energy of the system.

Q_q are the generalized forces.

q are the generalized coordinates.

For the double inverted rotary pendulum,

$$q = [\theta_1 \quad \theta_2 \quad \theta_3]^T \quad and$$

$$Qq = [\tau - b_1 \quad -b_2 \quad -b_3]^T \qquad \textit{Equation } 4.9$$

$$K = \frac{1}{2}J_1\dot{\theta}_1^2 + \frac{1}{2}J_2\dot{\theta}_2^2 + \frac{1}{2}J_3\dot{\theta}_3^2 + \frac{1}{2}m_2\left[\left(L_1\dot{\theta}_1 + L_2\dot{\theta}_2\cos\theta_2\right)^2 + \left(l_2\dot{\theta}_2\sin\theta_2\right)^2\right]$$

$$\frac{1}{2}m_3\left[\left(L_1\dot{\theta}_1 + L_2\dot{\theta}_2\cos\theta_2 + l_3\dot{\theta}_3\cos\theta_3\right)^2 + \left(L_2\dot{\theta}_2\sin\theta_2 + l_3\dot{\theta}_3\sin\theta_3\right)^2\right] \qquad \textit{Equation } 4.10$$

$$P = -\mathbf{g}m_2l_2\cos\theta_2 - \mathbf{g}m_3(l_2\cos\theta_2 + l_3\cos\theta_3) \qquad \textit{Equation } 4.11$$

Where,

m_i: is the mass of link *i*.

g: is the acceleration due to gravity.

L_i: is the length of link *i.*

l_i: is the length from the center of rotation of link *i* to its center of mass.

J_i is the moment of inertia about the center of rotation of link *i*.

θ_i is the angular coordinate of link *i.* Please refer to Figure 4.1.

τ is the control torque.

b_i is the viscous friction in the rotational joint of link *i*.

Applying the Euler Lagrange Equation to the Lagrangian results in three coupled non-linear equations substituting Equation 4.7 into Equation 4.8.

$$\frac{d}{dt}\frac{\partial L}{\partial \dot{\theta}_1} - \frac{\partial L}{\partial \theta_1} = \tau - b_1\dot{\theta}_1$$

becomes

$$\begin{aligned}\tau - b_1\dot{\theta}_1 &= J_1\ddot{\theta}_1 + m_2L_1\left[L_1\ddot{\theta}_1 + l_2\left(\ddot{\theta}_2\cos\theta_2 - \dot{\theta}_2^2\sin\theta_2\right)\right] \\ &\quad + m_3L_1\left[L_1\ddot{\theta}_1 + L_2\left(\ddot{\theta}_2\cos\theta_2 - \dot{\theta}_2^2\sin\theta_2\right) + l_3\left(\ddot{\theta}_3\cos\theta_3 - \dot{\theta}_3^2\sin\theta_3\right)\right] - 0 \\ &= \ddot{\theta}_1(J_1 + L_1^2(m_2 + m_3)) + L_1(m_2l_2 + m_3L_2)\ddot{\theta}_2\cos\theta_2 + m_3l_3L_1\ddot{\theta}_3\cos\theta_3 \\ &\quad - L_1(m_2l_2 + m_3L_2)\dot{\theta}_2^2\sin\theta_2 - m_3L_1l_3\dot{\theta}_3^2\sin\theta_3 \qquad \textit{Equation } 4.12\end{aligned}$$

and for θ_2

$$\frac{d}{dt}\frac{\partial L}{\partial \dot{\theta}_2} - \frac{\partial L}{\partial \theta_2} = -b_2\dot{\theta}_2$$

becomes

$$\begin{aligned}-b_2\dot{\theta}_2 &= (m_2l_2 + m_3L_2)L_1(\ddot{\theta}_1\cos\theta_2 - \dot{\theta}_1\dot{\theta}_2\sin\theta_2) + \ddot{\theta}_2(J_2 + m_2l_2^2 + m_3L_2^2) \\ &\quad + (\ddot{\theta}_3\cos(\theta_3 - \theta_2) - \dot{\theta}_3(\dot{\theta}_3 - \dot{\theta}_2)\sin(\theta_3 - \theta_2))m_3l_3L_2 \\ &\quad + (m_2l_2 + m_3L_2)L_1\dot{\theta}_1\dot{\theta}_2\sin\theta_2 - m_3l_3L_2\dot{\theta}_2\dot{\theta}_3\sin(\theta_3 - \theta_2) \\ &\quad + (m_2l_2 + m_3L_2)\mathbf{g}\sin\theta_2 \\ &= (m_2l_2 + m_3L_2)L_1\ddot{\theta}_1\cos\theta_2 + \ddot{\theta}_2(J_2 + m_2l_2^2 + m_3L_2^2) \\ &\quad + (\ddot{\theta}_3\cos(\theta_3 - \theta_2) - \dot{\theta}_3^2\sin(\theta_3 - \theta_2))m_3l_3L_2 + (m_2l_2 + m_3L_2)\mathbf{g}\sin\theta_2 \qquad \textit{Equation } 4.13\end{aligned}$$

and for θ_3

$$\frac{d}{dt}\frac{\partial L}{\partial \dot{\theta}_3} - \frac{\partial L}{\partial \theta_3} = -b_3\dot{\theta}_3$$

becomes

$$\begin{aligned}-b_3\dot{\theta}_3 &= m_3l_3L_1(\ddot{\theta}_1\cos\theta_3 - \dot{\theta}_1\dot{\theta}_3\sin\theta_3) + m_3l_3L_2(\ddot{\theta}_2\cos(\theta_3 - \theta_2) - \dot{\theta}_2(\dot{\theta}_3 - \dot{\theta}_2)\sin(\theta_3 - \theta_2)) \\ &\quad + \ddot{\theta}_3(J_3 + m_3l_3^2) + m_3l_3L_1\dot{\theta}_1\dot{\theta}_3\sin\theta_3 - m_3l_3L_2\dot{\theta}_2\dot{\theta}_3(\sin\theta_2\cos\theta_3 - \sin\theta_3\cos\theta_2)) \\ &\quad - m_3l_3^2\dot{\theta}_3^2(\sin\theta_3\cos\theta_3 - \sin\theta_3\cos\theta_3) + m_3\mathbf{g}l_3\sin\theta_3 \\ &= m_3l_3L_1\ddot{\theta}_1\cos\theta_3 + m_3l_3L_2(\ddot{\theta}_2\cos(\theta_3 - \theta_2) - \dot{\theta}_2(\dot{\theta}_3 - \dot{\theta}_2)\sin(\theta_3 - \theta_2) - \dot{\theta}_2\dot{\theta}_3\sin(\theta_2 - \theta_3)) \\ &\quad + \ddot{\theta}_3(J_3 + m_3l_3^2) + m_3\mathbf{g}l_3\sin\theta_3 \\ &= m_3l_3L_1\ddot{\theta}_1\cos\theta_3 + m_3l_3L_2(\ddot{\theta}_2\cos(\theta_3 - \theta_2) + \dot{\theta}_2^2\sin(\theta_3 - \theta_2)) + \ddot{\theta}_3(J_3 + m_3l_3^2) \\ &\quad + m_3\mathbf{g}l_3\sin\theta_3 \qquad \textit{Equation } 4.14\end{aligned}$$

If the equations are now parameterised they reduce to a more manageable form.

Defining $h_1, h_2, h_3, h_4, h_5, h_6, h_7,$ *and* h_8 *as*

$$h_1 = J_1 + L_1^2(m_2 + m_3)$$

$$h_2 = L_1(m_2 l_2 + m_3 L_2)$$

$$h_3 = L_1 m_3 l_3$$

$$h_4 = J_2 + L_2^2 m_3 + l_2^2 m_2$$

$$h_5 = L_2 m_3 l_3$$

$$h_6 = J_3 + l_3^2 m_3$$

$$h_7 = \mathbf{g}(m_2 l_2 + m_3 L_2)$$

$$h_8 = \mathbf{g} m_3 l_3$$

The dynamical equations reduce to

$$\tau - b_1\dot{\theta}_1 = h_1\ddot{\theta}_1 + h_2\ddot{\theta}_2\cos\theta_2 + h_3\theta_3\cos\theta_3 - h_2\dot{\theta}_2^2\sin\theta_2 - h_3\dot{\theta}_3^2\sin\theta_3$$

$$-b_2\dot{\theta}_2 = h_2\ddot{\theta}_1\cos\theta_2 + h_4\ddot{\theta}_2 + h_5\ddot{\theta}_3\cos(\theta_3 - \theta_2) - h_5\dot{\theta}_3^2\sin(\theta_3 - \theta_2) + h_7\sin\theta_2$$

$$-b_3\dot{\theta}_3 = h_3\ddot{\theta}_1\cos\theta_3 + h_5\ddot{\theta}_2\cos(\theta_3 - \theta_2) + h_6\ddot{\theta}_3 + h_5\dot{\theta}_2^2\sin(\theta_3 - \theta_2) + h_8\sin\theta_3$$

Equation 4.15

Which are the three nonlinear, coupled, second order differential equations of motion describing the dynamics of the double inverted rotary pendulum system.

4.2.3 Matlab Modelling

For the purpose of controller design and evaluation the single and double inverted pendulum systems were modelled in Matlab using Simulink.

The single and double inverted pendulums were modelled using a non-linear, parameterised Simulink model and an 'm file' as a run script for defining the physical parameters and control gains (see Appendix A). The Simulink models are as they appear in Figures 4.6 and 4.7.

From the Matlab models it was possible to build and test controllers for the pendulum systems and to optimise their performance before implementation on the actual pendulum equipment. This allowed faster development and the opportunity to investigate different methods of swing-up control.

For the Simulink Model, the nonlinear coupled equations of motion were rearranged to obtain an explicit form for the acceleration of each of the links. The output of this function was then fed through two integrators to obtain velocity and displacement. The resulting values for acceleration, velocity and displacement were then fed into a multiplexer and from there into the mathematical functions, namely the nonlinear equations of motion. (See Figure 4.6 and Figure 4.7.)

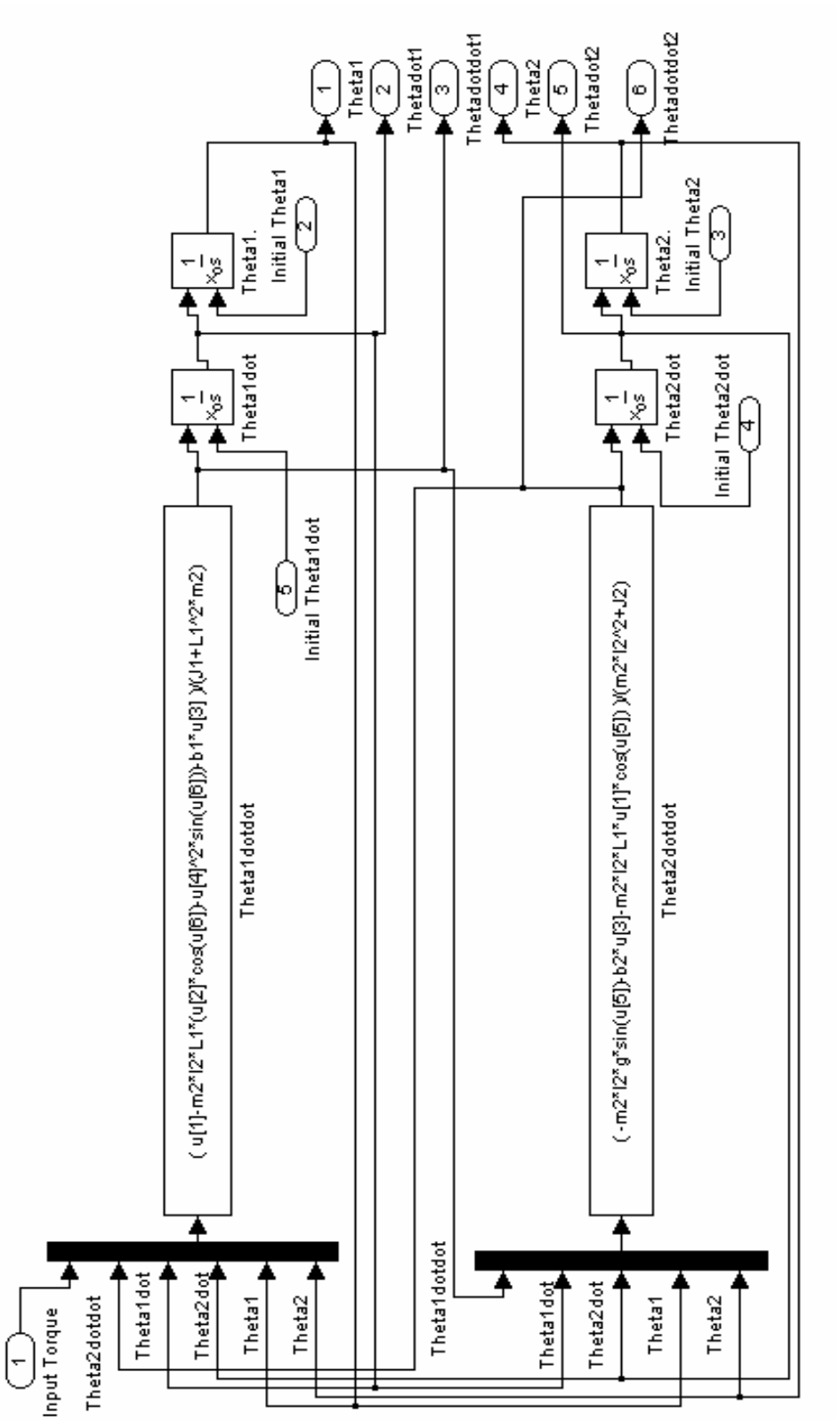

Figure 4.6 Simulink Model of the Single inverted rotary system

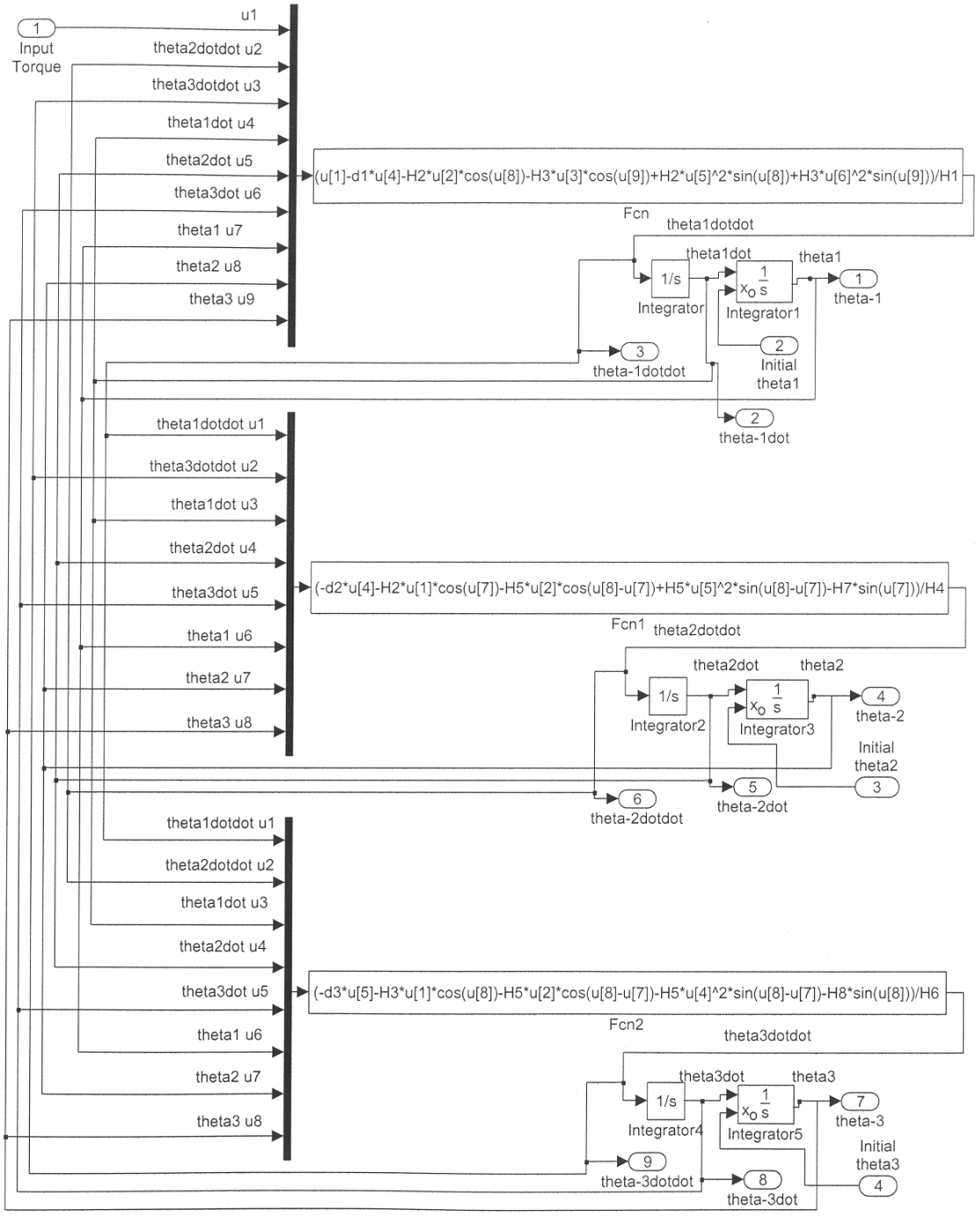

Figure 4.7 Simulink Model of the double inverted rotary pendulum system.

4.3 Virtual Reality Modelling

To help develop the mathematical model and test the control law, a virtual reality model of the double inverted pendulum has been created as shown in Figure 4.8. The model is a VRML file which is a basic approximation of the pendulum's geometry. It can be accessed in Simulink, where the signals labelled theta2 and theta3 in Figure 4.7 drive the virtual links' positions. This virtual model allows the designers to observe the system before it has been built. It has already been used to observe the mathematical model of the system. It could also be used to follow actual system behaviour where the input to the virtual pendulum comes directly from system measurements. It was anticipated that the virtual pendulum could later be used in running real time simulations.

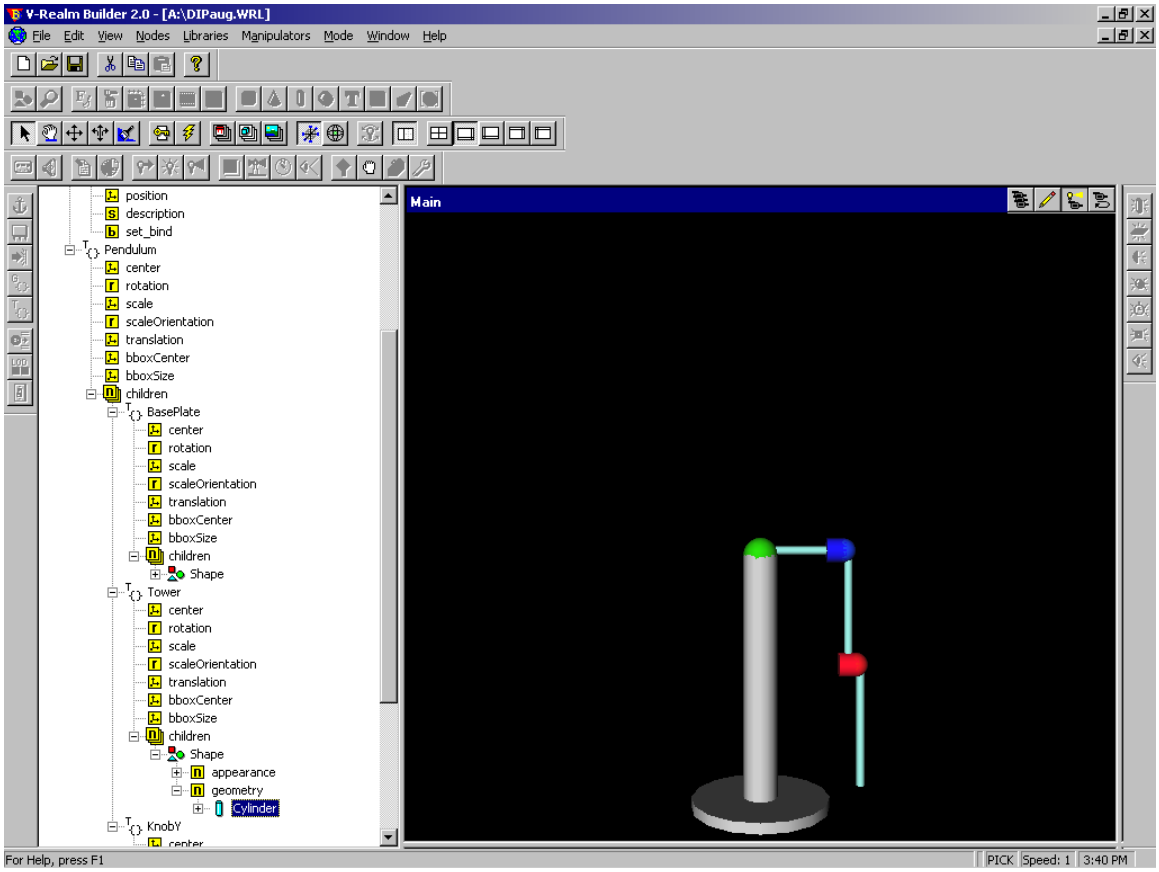

Figure 4.8 Screen shot of the virtual pendulum in V-realm builder

5. SYSTEM IDENTIFICATION

To implement the controllers as designed using the mathematical models, the real parameters of the system needed to be determined accurately.

The majority of the parameters describing the system were determined accurately from the mechanical drawings, material properties and data sheets for the respective components. However the viscous damping of the first and second pendulum links had to be determined experimentally.

5.1 Component Parameters

The component parameters are as follows in Table 5.1 from the component data sheets. Table 5.2 lists the parameters of the designed and built components.

Table 5.1 Component parametric data.

Item	Moment of Inertia (kgm^2) (Rotating Parts)	Mass (kg)	Moment of inertia (Stationary Parts)	Model/ Code
Encoder	$<10^{-6}$	0.078	Not Given	Omron: E6B2
Servo Motor	$2.14x10^{-5}$	0.9	Not Required	RS 263-5995

Table 5.2 Designed and built component parametric data.

Item	Moment of Inertia (kgm^2) about centre of rotation	Mass (kg)	Distance to centre of mass from rotational centre (m)
Manual input knob.	N/A	N/A	N/A
Horizontal link.	$1.67x10^{-4}$	0.050	0.120
Encoder housing for first pendulum encoder.	$1.36x10^{-4}$	0.187	0.250
Encoder to link joint for the first pendulum.	$3.577x10^{-6}$	0.045	0.310
Link joint cover.	N/A	N/A	N/A
First pendulum link.	$2.22x10^{-3}$	0.075	0.148
Encoder housing for second pendulum encoder.	$1.69X10^{-4}$	0.187	0.298
Encoder to link joint for the second pendulum encoder.	$3.19*10^{-6}$	0.030	0.313
Link joint cover.	N/A	N/A	N/A
Second pendulum link.	$3.58x10^{-3}$	0.088	0.152

Once all of the part parameters were known they could to be used to calculate the parameters used in the Matlab scripts for the inverted pendulum.

The starting point was the single inverted pendulum for which the parameters are,

m_2 the mass of the pendulum (kg)

b_1 the friction of the motor rotor (Nms)

b_2 the friction of the pendulum (Nms)

l_2 the length to pendulum centre of mass (kg)

L_1 the length of horizontal link (m)

J_1 the inertia of the horizontal link (kgm^2)

J_2 the inertia of the pendulum (kgm^2) (including encoder and housing)

g the acceleration due to gravity m/s^2 assumed as 9.8 m/s^2

For the double inverted pendulum these parameters are,

L_1 the length of horizontal link (m)

L_2 the length of middle link or first pendulum link (m)

l_2 the distance from centre of rotation of middle link to its centre of gravity (m)

l_3 the distance from the centre of rotation of the end link to its centre of gravity (m)

m_2 the mass of link 2 (kg)

m_3 the mass of link 3 (kg)

J_1 the inertia of link 1 about its centre of rotation (kgm^2)

J_2 the inertia of link 2 about its centre of gravity (kgm^2)

J_3 the inertia of link 3 about its centre of gravity (kgm^2)

b_1 the damping in motor bearings (Nms)

b_2 the damping in the first encoder bearing (Nms) (encoder supporting middle link)

b_3 the damping in the second encoder bearing (Nms)

g the acceleration due to gravity (m/s^2) assumed as 9.8 m/s^2

To determine the moments of inertia the parallel axis theorem and the information obtained from Solid Edge™ was used.

The parallel axis theorem is as follows,

$J_{Parallel\ Axis} = I_{centroidal\ Axis} + md^2$ (Efunda, 2004)

Using this information Table 5.3 was generated. Note that the single inverted pendulum rig is formed by detaching the second pendulum link and the second encoder housing.

Table 5.3 Physical parameters of the single and double inverted pendulum rigs.

Parameter (Single inverted pendulum)	Numeric Value	Unit	Parameter (Double inverted pendulum)	Numeric Value	Unit
m2	0.075	kg	m2	0.370	kg
b1	0.0001	Nms	m3	0.088	kg
b2	0.00028	Nms	b1	0.0001	Nms
l2	0.148	m	b2	0.00028	Nms
L1	0.278	m	b3	0.00028	Nms
J1	2.48E-02	kgm2	l2	0.269	m
J2	3.86E-03	kgm2	l3	0.152	m
g	9.8	m/s2	L1	0.278	m
			L2	0.313	m
			J1	2.48E-02	kgm2
			J2	3.04E-02	kgm2
			J3	5.61E-03	kgm2
			g	9.8	m/s2

To complete the system knowledge it was also necessary to determine the damping of the rotating joints. The damping of the motor was calculated from information on the data sheet and the equations of motion for a DC constant field motor.

The equations of motion for a DC motor are as shown in Equation 5.1 (Wolfman, 2004).

$$J\ddot{\theta} + b\dot{\theta} = Ki\ , \quad L\frac{di}{dt} + Ri = V - K\dot{\theta}$$

Where

J *is the rotor inertia* (kgm^2 / s^2)

$\dot{\theta}$ *is the angular position* (*radians*)

b *is the damping* (*Nms*)

K *is the motor* constant (Nm / amp)

i *is the current flowing through the motor* (*amps*)

L *is the motor* inductance (H)

R *is the motor* resistance (*ohm*)

V *is the applied voltage* (*Volts*) *Equation* 5.1

To derive the system damping it was realised that at no load steady state conditions Equation 5.1 reduced to Equation 5.2.

$$b\dot{\theta} = Ki\ , \quad Ri = V - K\dot{\theta} \text{ as the system is assumed steady state}$$

$$\text{or } b = \frac{K(V - K\dot{\theta})}{\dot{\theta}\ R} \qquad \textit{Equation } 5.2$$

From the motor data sheet the parameters of interest are, at no load conditions,

K = 0.09 Nm/amp

V = 24 volts

R = 7.8 ohms

$\dot{\theta}$ = 2300 rpm or 240 rad/sec

Which results in a damping b = 0.0001 Nm/s

The damping of the encoder bearings and the data couple link were determined through measurement. This was done by measuring the logarithmic decrement of the pendulum with the data couple engaged and disengaged. Measuring the logarithmic decrement relates successive peak values of displacement to the damping ratio, which was then used to calculate the viscous damping coefficient of the bearings / data couple. This approach is only valid within the linear range of the system (where the natural frequency of small perturbations is valid) and assumes no stiction (static friction).

The logarithmic decrement is defined as (Zander, 2004),

$$\delta = \frac{1}{n}\ln\left(\frac{x_i}{x_{i+n}}\right) \quad \textit{where,} \qquad \textit{Equation } 5.3$$

δ *is the* logarithmic *decrement*
x_i *is the displacement amplitude at peak i*
n is some finite number equal to or greater than one

This can be related to bearing damping with the Equation 5.4 (Vibrations, 2004),

$$b = \frac{2\sqrt{km}\delta}{\sqrt{4\pi^2 + \delta^2}} \quad \textit{where,} \qquad \textit{Equation } 5.4$$

b is bearing damping
k is the equivalent spring stiffness
m is the equivalent mass and
δ *is the* logarithmic *decrement as before*

Realising that for the pendulum system k and m are m_2gl_2 and J_2 respectively Equation 5.4 is rewritten as Equation 6.5,

$$b = \frac{2\sqrt{m_2 l_2 \mathbf{g} J_2}\,\delta}{\sqrt{4\pi^2 + \delta^2}} \quad \textit{where,} \qquad \textit{Equation } 5.5$$

Equation 5.5 allows the experimental data to be computed to reveal the damping properties of the encoder alone and the encoder plus data couple link, although it should be noted that the significant stiction lead to unreliable results for the data couple engaged configuration. This data could then be input into the run script to generate the correct control gains for both the single and double inverted pendulum systems.

Experimental data is presented in Table 5.4.

Table 5.4 Damping measurements of the encoder bearings and the encoder bearings plus data couple.

Encoder plus data couple bearing damping			
t_i (s)	θ_i (radians)	δ (dimensionless)	b (Nms)
$t_0 = 6.64$	$\theta_0 = 0.265$	N/A	
$t_1 = 7.51$	$\theta_1 = 0.187$	0.348	
$t_2 = 8.38$	$\theta_2 = 0.111$	0.521	
	Average	0.435	0.0028
(Note that since the friction was so great only three measurements were possible within the region of linearity)			
Encoder bearing damping			
t_i (s)	θ_i (radians)	δ (dimensionless)	b (Nms)
$t_0 = 0.60$	$\theta_0 = 0.1288$		
$t_1 = 1.47$	$\theta_1 = 0.1241$	0.0372	
$t_2 = 2.35$	$\theta_2 = 0.1194$	0.0386	
$t_3 = 3.22$	$\theta_3 = 0.1147$	0.0401	
$t_4 = 4.09$	$\theta_4 = 0.1100$	0.0418	
$t_5 = 4.96$	$\theta_5 = 0.1052$	0.0446	
$t_6 = 5.83$	$\theta_6 = 0.1005$	0.0457	
$t_7 = 6.70$	$\theta_7 = 0.0958$	0.0479	
$t_8 = 7.47$	$\theta_8 = 0.0911$	0.0503	
$t_9 = 8.44$	$\theta_9 = 0.0880$	0.0346	
$t_{10} = 9.32$	$\theta_{10} = 0.0833$	0.0548	
	Arithmetic Average	0.0437	0.00028
	(n=10) (See Equation 5.3)	0.0436	0.00028

6. CONTROLLER DESIGN

One of the major focuses of the inverted pendulum project was to develop control strategies to make the upright equilibria asymptotically stable. This would involve first displacing the pendulum(s) from its stable equilibria and driving it towards the unstable equilibria.

To achieve asymptotic stability of the upright (unstable) equilibrium position a number of approaches were taken. These will be addressed in the following sections, beginning with the single inverted pendulum and finally the double inverted pendulum.

6.1 Single Inverted Pendulum

The model of the single inverted pendulum was used as a testing medium for methods of stabilisation which may also work on the double inverted pendulum. The control methodologies successfully implemented on the single inverted pendulum model include a linear quadratic regulator (optimal controller) regulating about the upright equilibrium within domain of attraction and various swing-up strategies.

The swing up strategies successfully implemented on the single inverted pendulum model were an energy based method of swing up control and an array of constant gain controllers regulating about an arbitrary set point.

6.1.1 Linear Quadratic Regulator for the Single Inverted Pendulum

The linear quadratic regulator (LQR) was used to regulate about the upright equilibrium point. As the name may suggest the LQR controller requires a linear system for which it will generate constant gains for full state feedback to make the equilibrium point globally asymptotically stable. However the dynamics of inverted pendulum systems are inherently nonlinear. This leaves the problem of how to implement a control methodology designed for a linear system on a nonlinear system. The chosen approach was to linearise the equations of motion about the operating point and define a domain of attraction within which the constant gain controller results in local asymptotic stability. Delivering the system to the domain of attraction was achieved by a different method.

Within the realms of Matlab a full state feedback LQR controller is developed by solving the Algebraic Ricatti Equation based upon an effort weighting matrix and a

state penalty matrix. For this the nonlinear dynamical equations must be written in the linear state space format. Further, it should be noted that the resulting LQR regulates only about a zero equilibrium. Since the equations of motion are not zero about the desired operating point and that in general the upright equilibrium can be described by an infinite number of coordinates, some kind of filtering of the signal passed to the constant gain controller is needed.

First the state space model was derived as follows. Recall the second order nonlinear coupled differential equations describing the dynamics of the single inverted pendulum.

$$\ddot{\theta}_1(J_1 + L_1^2 m_2) = \tau - m_2 l_2 L_1(\ddot{\theta}_2 \cos\theta_2 - \dot{\theta}_2^2 \sin\theta_2) - b_1\dot{\theta}_1 \qquad \textit{Equation } 4.6$$

$$\ddot{\theta}_2(m_2 l_2^2 + J_2) = -m_2 l_2 \mathrm{g} \sin\theta_2 - b_2\dot{\theta}_2 - m_2 l_2 L_1 \ddot{\theta}_1 \cos\theta_2 \qquad \textit{Equation } 4.5$$

Where

J_1 *is the moment of inertia of link* 1 *about its center of rotation*

J_2 *is the moment of inertia of link* 2 *about its center of mass*

L_1 *is the length of link* 1

l_2 *is the length between the center of mass and the center of rotation in linnk* 2

m_2 *is the mass of link* 2

b_1 *is the coefficient of friction of the bearing about which link* 1 *rotates*

b_2 *is the coefficient of friction of the bearing about which link* 2 *rotates*

g *is the acceleration due to gravity*

If it is assumed that at the equilibrium point,

$$\theta_2 = \pi + \delta$$
$$\dot{\theta}_2^2 = 0$$
$$\sin\theta_2 = -\delta$$
$$\cos\theta_2 = -1$$

Then the equations of motion reduce to,

$$\ddot{\theta}_1(J_1 + L_1^2 m_2) = \tau + m_2 l_2 L_1 \ddot{\theta}_2 - b_1\dot{\theta}_1 \qquad \textit{Equation } 6.1$$

$$\ddot{\theta}_2(m_2 l_2^2 + J_2) = -m_2 l_2 \mathrm{g}(\pi - \theta_2) - b_2\dot{\theta}_2 + m_2 l_2 L_1 \ddot{\theta}_1 \qquad \textit{Equation } 6.2$$

The linearised equations can then be written in matrix form as,

$$\begin{bmatrix} \tau \\ 0 \end{bmatrix} = \begin{bmatrix} J_1 + L_1^2 m_2 & -m_2 l_2 L_1 \\ -m_2 l_2 L_1 & m_2 l_2^2 + J_2 \end{bmatrix} \begin{bmatrix} \ddot{\theta}_1 \\ \ddot{\theta}_2 \end{bmatrix} + \begin{bmatrix} b_1\dot{\theta}_1 \\ b_2\dot{\theta}_2 + m_2 l_2 \mathrm{g}(\pi - \theta_2) \end{bmatrix} \qquad \textit{Equation } 6.3$$

Which rearranges to

$$\begin{bmatrix} J_1 + L_1^2 m_2 & -m_2 l_2 L_1 \\ -m_2 l_2 L_1 & m_2 l_2^2 + J_2 \end{bmatrix} \begin{bmatrix} \ddot{\theta}_1 \\ \ddot{\theta}_2 \end{bmatrix} = \begin{bmatrix} \tau - b_1\dot{\theta}_1 \\ -b_2\dot{\theta}_2 - m_2 l_2 \mathrm{g}(\pi - \theta_2) \end{bmatrix}$$

Again rearanging

$$\begin{bmatrix} \ddot{\theta}_1 \\ \ddot{\theta}_2 \end{bmatrix} = \begin{bmatrix} m_2 l_2^2 + J_2 & m_2 l_2 L_1 \\ m_2 l_2 L_1 & J_1 + L_1^2 m_2 \end{bmatrix} \begin{bmatrix} \tau - b_1\dot{\theta}_1 \\ -b_2\dot{\theta}_2 - m_2 l_2 \mathrm{g}(\pi - \theta_2) \end{bmatrix} / [(J_1 + L_1^2 m_2)(m_2 l_2^2 + J_2) - (m_2 l_2 L_1)^2]$$

Which yeilds the following state space representation

$$\begin{bmatrix} \dot{\theta}_1 \\ \dot{\theta}_2 \\ \ddot{\theta}_1 \\ \ddot{\theta}_2 \end{bmatrix} = \begin{bmatrix} 0 & 0 & 1 & 0 \\ 0 & 0 & 0 & 1 \\ 0 & \left(m_2^2 l_2^2 L_1 \mathrm{g}\right)/A & -b_1\left(m_2 l_2^2 + J_2\right)/A & -b_2 m_2 l_2 L_1 / A \\ 0 & (J_1 + L_1^2 m_2) m_2 l_2 \mathrm{g} / A & -m_2 l_2 L_1 b_1 / A & -b_2(J_1 + L_1^2 m_2)/A \end{bmatrix} \begin{bmatrix} \theta_1 \\ \theta_2 \\ \dot{\theta}_1 \\ \dot{\theta}_2 \end{bmatrix} + \begin{bmatrix} 0 \\ 0 \\ (m_2 l_2^2 + J_2)/A \\ m_2 l_2 L_1 / A \end{bmatrix} \tau$$

With

$$A = [(J_1 + L_1^2 m_2)(m_2 l_2^2 + J_2) - (m_2 l_2 L_1)^2] \qquad \textit{Equation } 6.4$$

Once the linearised state space representation of the pendulum was obtained the parameters could then be put into the Matlab script shown in Appendix A, and the control gains derived and fed into the Simulink model for verification.

6.1.2 Swing-Up Control for the Single Inverted Pendulum

To achieve global asymptotic stability it was necessary to include some form of controller to deliver the system to the domain of attraction about which the linearised state space controller would achieve stability.

There were two methods of swing up control investigated which yielded successful simulation results. These methods were a gain scheduling method and an energy based swing-up method.

6.1.2.1 Energy Control

The objective of energy control in the context of this text is simply to regulate the total system energy to be that of the static upright equilibrium. To achieve energy control energy needs to fed into the system equal to that of the static upright equilibrium position and to switch to stabilisation control once the system reaches the domain of attraction. By domain of attraction it is meant that link velocities must be sufficiently small and the pendulum must be sufficiently close to the upright position. Such a method of control is often referred to as a "bang-bang" method (Åström and Furuta, 1996).

To implement a swing-up strategy as such one requires conditions for increasing energy in the system and a switching mechanism to switch between the control strategies.

The derivation of these conditions is as follows. The total energy equation is defined and then differentiated with respect to time and the conditions for energy increase over time implied.

First define the total energy equation of the system.

$E_{tot} = K + P$

Where

E_{tot} *is the total system energy*

K *is the Kinetic Energy and*

P *is the Potential Energy*

$$K = \frac{1}{2}J_1\dot{\theta}_1^2 + \frac{1}{2}J_2\dot{\theta}_2^2 + \frac{1}{2}m_2[(L_1\dot{\theta}_1 + l_2\dot{\theta}_2\cos\theta_2)^2 + (l_2\dot{\theta}_2\sin\theta_2)^2] \qquad \textit{Equation } 6.5$$

$$P = -gm_2l_2\cos\theta_2 \qquad \textit{Equation } 6.6$$

With parameters as defined in Section 6.1.1

At this point it is noted that for the purpose of the derivation of the conditions for energy input the dynamics of the horizontal link can be ignored and only the acceleration of the pivot point of the pendulum link considered. In this case the energy equation simplifies to,

$$E_{tot} = \frac{1}{2}J_2\dot{\theta}_2^2 + \frac{1}{2}m_2[(l_2\dot{\theta}_2\cos\theta_2)^2 + (l_2\dot{\theta}_2\sin\theta_2)^2] - gm_2l_2\cos\theta_2$$

$$= \frac{1}{2}J_2\dot{\theta}_2^2 + \frac{1}{2}m_2l_2^2\dot{\theta}_2^2 - gm_2l_2\cos\theta_2 \qquad \textit{Equation } 6.7$$

Taking the derivative with respect to time we get

$$\frac{\partial E_{tot}}{\partial t} = J_2\dot{\theta}_2\ddot{\theta}_2 + m_2l_2^2\dot{\theta}_2\ddot{\theta}_2 + gm_2l_2\dot{\theta}_2\sin\theta_2$$

substituting in Equation 4.6 *and ignoring friction*, $\dot{\theta}_1$ *and* θ_1 *we get*

$$\frac{\partial E_{tot}}{\partial t} = \dot{\theta}_2(-m_2l_2L_1\ddot{\theta}_1\cos\theta_2) \qquad \textit{Equation } 6.8$$

Equation 6.8 implies that to increase system energy the input torque should be opposite in sign to the expression $\dot{\theta}_2\cos\theta_2$.

With the requirements for energy increase in the system defined, it was necessary to define the criterion for switching energy input on and off. The energy of the system is defined by the total energy equation (Equation 6.7) and a logic switch should be used to turn the energy input off once the system energy is equal to the upright static equilibrium.

$$E_{tot} = \frac{1}{2}J_1\dot{\theta}_1^2 + \frac{1}{2}J_2\dot{\theta}_2^2 + \frac{1}{2}m_2[(L_1\dot{\theta}_1 + l_2\dot{\theta}_2\cos\theta_2)^2 + (l_2\dot{\theta}_2\sin\theta_2)^2] - gm_2l_2\cos\theta_2$$

and

$E_{tot} = gm_2l_2$ *at the upright static equilibrium.* *Equation* 6.9

To implement this strategy in Matlab a logic switch was implemented to switch between swing up and stabilisation control. The Simulink model is as shown in Figure 6.1

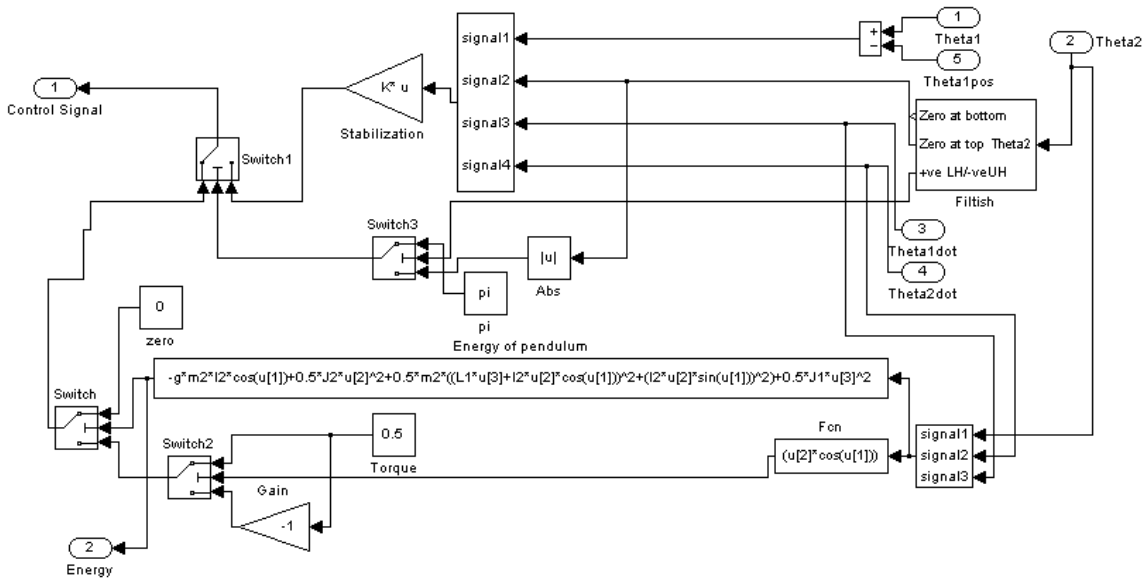

Figure 6.1 Simulink model of energy based controller.

Once the physical parameters were implemented and system simulations performed it was noted that the horizontal link moved outside the physical limits of the rig and that much of the energy was manifesting itself in the kinetic energy of the horizontal link. This was not a desirable result. One solution that the authors discovered was that by ensuring that control torque pushed the horizontal link towards zero the link velocity was reduced and the link remained close to the zero point. Such a strategy was achieved by adding an extra piece of logic allowing energy input to occur only when the required torque was in the direction that would drive the horizontal link toward zero. This strategy is shown in Figure 6.2 (look to Fcn1 on the figure).

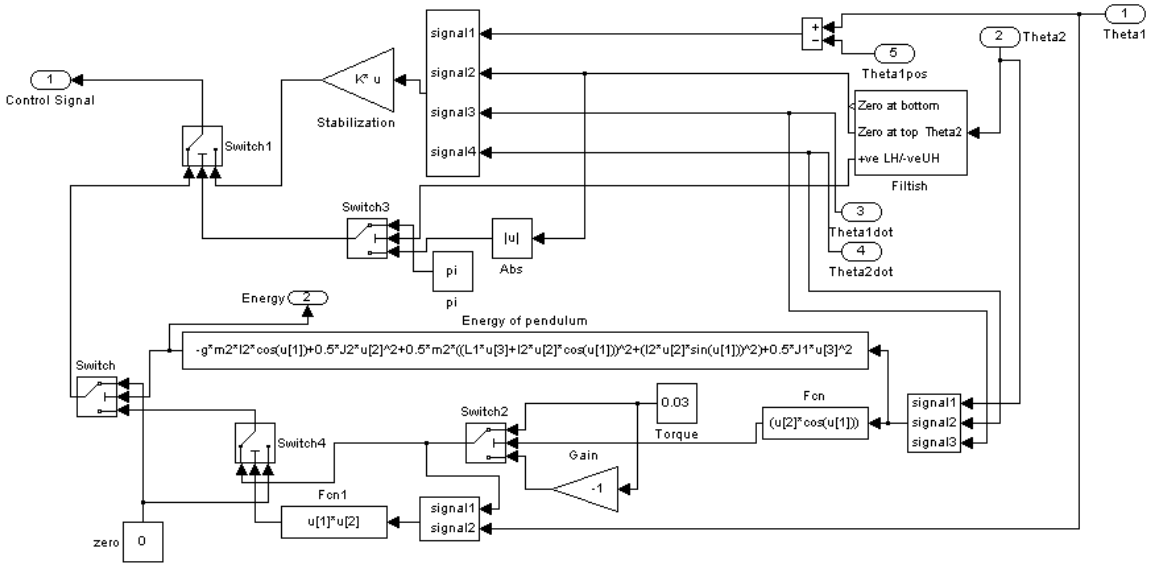

Figure 6.2 Simulink model of energy based controller with additional logic.

The resulting control system using this energy control plus the additional logic to drive the horizontal link to the zero dynamic position was more robust and stayed within the physical limits of the system in simulation.

6.1.2.2 Gain Scheduling Control

The approach of control referred to as gain scheduling is usually applied to an array of linear controllers that regulate around a predetermined trajectory. The immediate draw back of such a system is that the initial conditions must be always the same for swing-up control to work or alternatively a large array of different controllers for each trajectory from every possible set of initial conditions.

For the single inverted pendulum a slightly alternative approach was taken to assess the feasibility of success. An array of constant gain controllers assuming zero velocities and pseudo equilibrium torques was implemented and a reference trajectory applied to the pendulum angle. Although successful in Matlab simulations the results showed large control signals were required. The layout of this system in Simulink is as follows in Figure 6.3.

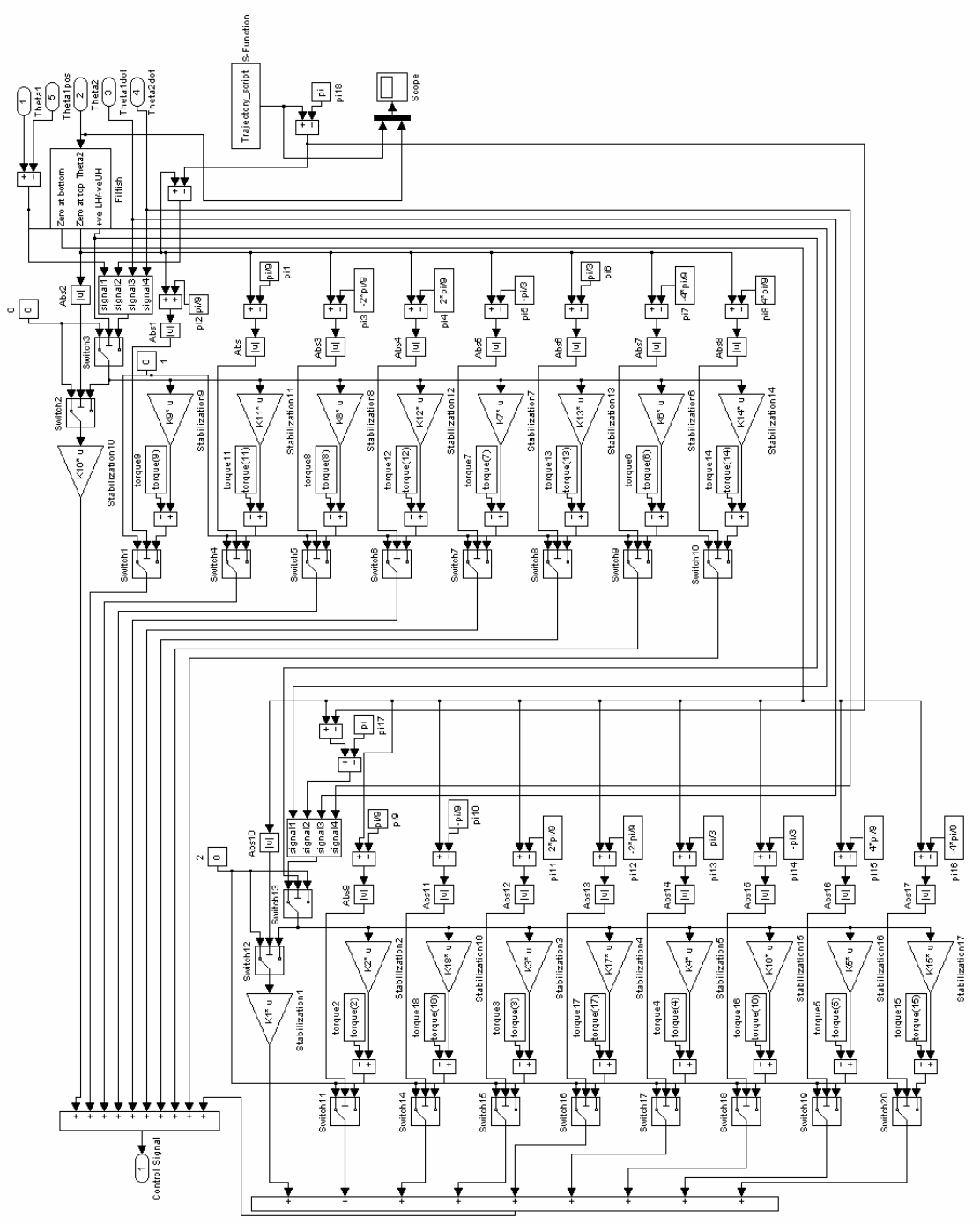

Figure 6.3 Simulink model of gain scheduling controller.

To linearise the equations of motion a Taylor expansion about a general operating point was undertaken. The resulting mathematics is as follows. (See Appendix B for Taylor series.)

Recall the second order nonlinear coupled differential equations describing the dynamics of the single inverted pendulum.

$$\ddot{\theta}_1(J_1 + L_1^2 m_2) = \tau - m_2 l_2 L_1(\ddot{\theta}_2 \cos\theta_2 - \dot{\theta}_2^2 \sin\theta_2) - b_1\dot{\theta}_1 \qquad \textit{Equation } 4.6$$

$$\ddot{\theta}_2(m_2 l_2^2 + J_2) = -m_2 l_2 \mathrm{g} \sin\theta_2 - b_2\dot{\theta}_2 - m_2 l_2 L_1 \ddot{\theta}_1 \cos\theta_2 \qquad \textit{Equation } 4.5$$

Where

J_1 *is the moment of inertia of link* 1 *about its center of rotation*

J_2 *is the moment of inertia of link* 2 *about its center of mass*

L_1 *is the length of link* 1

l_2 *is the length between the center of mass and the center of rotation in linnk* 2

m_2 *is the mass of link* 2

b_1 *is the coefficient of friction of the bearing about which link* 1 *rotates*

b_2 *is the coefficient of friction of the bearing about which link* 2 *rotates*

g *is the acceleration due to gravity*

Let Equations 4.6 *and* 4.7 *be rewritten as Equation* 6.10 (*below*)

$$\ddot{\theta}_1 = \frac{(m_2 l_2^2 + J_2)(\tau + m_2 l_2 L_1 \dot{\theta}_2^2 \sin\theta_2 - b_1\dot{\theta}_1) + m_2 l_2 L_1 \cos\theta_2 (m_2 l_2 \mathrm{g} \sin\theta_2 + b_2\dot{\theta}_2)}{(J_1 + m_2 L_1^2)(J_2 + m_2 l_2^2) - (m_2 l_2 L_1 \cos\theta_2)^2}$$

$$\ddot{\theta}_2 = \frac{-m_2 l_2 L_1 \cos\theta_2 (\tau + m_2 l_2 L_1 \dot{\theta}_2^2 \sin\theta_2 - b_1\dot{\theta}_1) - (J_1 + m_2 L_1^2)(m_2 l_2 \mathrm{g} \sin\theta_2 + b_2\dot{\theta}_2)}{(J_1 + m_2 L_1^2)(J_2 + m_2 l_2^2) - (m_2 l_2 L_1 \cos\theta_2)^2}$$

The first step was to take the partial derivatives of the two non-linear equations of motion with respect to all of the state variables. The result was,

$$\frac{\partial \ddot{\theta}_1}{\partial \theta_2} = \frac{(m_2 l_2^2 + J_2) m_2 l_2 L_1 \dot{\theta}_2^2 \cos\theta_2 - (m_2 l_2 \sin\theta_2)^2 L_1 - m_2 l_2 L_1 b_2 \dot{\theta}_2 \sin\theta_2 + (m_2 l_2 \cos\theta_2)^2 L_1 \mathrm{g}}{(J_1 + m_2 L_1^2)(J_2 + m_2 l_2^2) - (m_2 l_2 L_1 \cos\theta_2)^2}$$

$$- \frac{2 m_2 l_2 L_1 \cos\theta_2 \sin\theta_2}{(J_1 + m_2 L_1^2)(J_2 + m_2 l_2^2) - (m_2 l_2 L_1 \cos\theta_2)^2} \ddot{\theta}_1$$

$$\frac{\partial \ddot{\theta}_1}{\partial \dot{\theta}_1} = \frac{-b_1 (m_2 l_2^2 + J_2)}{(J_1 + m_2 L_1^2)(J_2 + m_2 l_2^2) - (m_2 l_2 L_1 \cos\theta_2)^2}$$

$$\frac{\partial \ddot{\theta}_1}{\partial \dot{\theta}_2} = \frac{2 m_2 l_2 L_1 \dot{\theta}_2 \sin\theta_2 (m_2 l_2^2 + J_2) + m_2 l_2 L_1 b_2 \cos\theta_2}{(J_1 + m_2 L_1^2)(J_2 + m_2 l_2^2) - (m_2 l_2 L_1 \cos\theta_2)^2}$$

$$\frac{\partial \ddot{\theta}_1}{\partial \tau} = \frac{(m_2 l_2^2 + J_2)}{(J_1 + m_2 L_1^2)(J_2 + m_2 l_2^2) - (m_2 l_2 L_1 \cos\theta_2)^2} \qquad \textit{Equation } 6.11$$

For the horizontal (driven) link and,

$$\frac{\partial \ddot{\theta}_2}{\partial \theta_2} = \frac{(m_2 l_2 L_1 \dot{\theta}_2)^2(\sin^2\theta_2 - \cos^2\theta_2) + m_2 l_2 L_1 \sin\theta_2(\tau - b_1\dot{\theta}_1) - (J_1 + m_2 L_1^2)m_2 l_2 \mathrm{g}\cos\theta_2}{(J_1 + m_2 L_1^2)(J_2 + m_2 l_2^2) - (m_2 l_2 L_1 \cos\theta_2)^2}$$
$$- \frac{2m_2 l_2 L_1 \cos\theta_2 \sin\theta_2}{(J_1 + m_2 L_1^2)(J_2 + m_2 l_2^2) - (m_2 l_2 L_1 \cos\theta_2)^2}\ddot{\theta}_2$$
$$\frac{\partial \ddot{\theta}_2}{\partial \dot{\theta}_1} = \frac{b_1 m_2 l_2 L_1 \cos\theta_2}{(J_1 + m_2 L_1^2)(J_2 + m_2 l_2^2) - (m_2 l_2 L_1 \cos\theta_2)^2}$$
$$\frac{\partial \ddot{\theta}_2}{\partial \dot{\theta}_2} = \frac{2(m_2 l_2 L_1)^2 \dot{\theta}_2 \sin\theta_2 \cos\theta_2 - b_2(J_1 + m_2 L_1^2)}{(J_1 + m_2 L_1^2)(J_2 + m_2 l_2^2) - (m_2 l_2 L_1 \cos\theta_2)^2}$$
$$\frac{\partial \ddot{\theta}_2}{\partial \tau} = \frac{-m_2 l_2 L_1 \cos\theta_2}{(J_1 + m_2 L_1^2)(J_2 + m_2 l_2^2) - (m_2 l_2 L_1 \cos\theta_2)^2}$$

Equation 6.12

for the pendulum link.

To realise this in state space it was recognised that about the operating point, the state space equations would be the product of the first partial derivatives with respect to each independent variable with that independent variable.

$$\begin{bmatrix} \dot{\theta}_1 \\ \dot{\theta}_2 \\ \ddot{\theta}_1 \\ \ddot{\theta}_2 \end{bmatrix} = \begin{bmatrix} 0 & 0 & 1 & 0 \\ 0 & 0 & 0 & 1 \\ 0 & \frac{\partial \ddot{\theta}_1}{\partial \theta_2} & \frac{\partial \ddot{\theta}_1}{\partial \dot{\theta}_1} & \frac{\partial \ddot{\theta}_1}{\partial \dot{\theta}_2} \\ 0 & \frac{\partial \ddot{\theta}_2}{\partial \theta_2} & \frac{\partial \ddot{\theta}_2}{\partial \dot{\theta}_1} & \frac{\partial \ddot{\theta}_2}{\partial \dot{\theta}_2} \end{bmatrix} \begin{bmatrix} \theta_1 \\ \theta_2 \\ \dot{\theta}_1 \\ \dot{\theta}_2 \end{bmatrix} + \begin{bmatrix} 0 \\ 0 \\ \frac{\partial \ddot{\theta}_1}{\partial \tau} \\ \frac{\partial \ddot{\theta}_2}{\partial \tau} \end{bmatrix} \tau$$

Equation 6.13

It should be noted that state space assumes zero equilibrium to be the operating point so to implement this state space form the input signals have to be conditioned to reflect the zero equilibrium assumption. This resulted in signal conditioning for each linearised controller.

6.1.3 Command Tracking Single Inverted Pendulum

A further point of interest for the inverted pendulum control was to have command tracking so that the horizontal link could be positioned anywhere between the physical bounds once the pendulum was in the inverted position. This was achieved by adding an offset to the measured angle of the horizontal link to make the LQR regulate about a different zero point.

6.2 Double Inverted Pendulum

Dynamically the double inverted pendulum is the same as the single inverted pendulum with an extra un-actuated degree of freedom.

6.2.1 Linear Quadratic Regulator for the Double Inverted Pendulum

The linear quadratic regulator (LQR) was used to regulate about the upright equilibrium point. As the name may suggest the LQR controller requires a linear system for which it will generate constant gains for full state feedback to make the equilibrium point globally asymptotically stable. However the dynamics of inverted pendulum systems are inherently nonlinear. This leaves the problem of how to implement a control methodology designed for a linear system on a nonlinear system. The chosen approach was to linearise the equations of motion about the operating point and define a domain of attraction within which the constant gain controller results in local asymptotic stability. Delivering the double pendulum system to the domain of attraction was not achieved. Another method is required, and outside the scope of this project.

Within the realms of Matlab a full state feedback LQR controller is developed by solving the Algebraic Ricatti Equation based upon an effort weighting matrix and a state penalty matrix. For this the nonlinear dynamic equations must be written in the linear state space format. A further point of note is that the resulting LQR regulates only about a zero equilibrium. Since the equations of motion are not zero about the desired operating point and that in general the upright equilibrium can be described by an infinite number of coordinates some kind of conditioning of the signal passed to the constant gain controller is needed.

First the state space model was derived as follows. Recall the second order nonlinear coupled differential equations describing the dynamics of the double inverted pendulum (Equation 4.16).

$$\tau - b_1\dot{\theta}_1 = h_1\ddot{\theta}_1 + h_2\ddot{\theta}_2\cos\theta_2 + h_3\theta_3\cos\theta_3 - h_2\dot{\theta}_2^2\sin\theta_2 - h_3\dot{\theta}_3^2\sin\theta_3$$
$$-b_2\dot{\theta}_2 = h_2\ddot{\theta}_1\cos\theta_2 + h_4\ddot{\theta}_2 + h_5\ddot{\theta}_3\cos(\theta_3 - \theta_2) - h_5\dot{\theta}_3^2\sin(\theta_3 - \theta_2) + h_7\sin\theta_2$$
$$-b_3\dot{\theta}_3 = h_3\ddot{\theta}_1\cos\theta_3 + h_5\ddot{\theta}_2\cos(\theta_3 - \theta_2) + h_6\ddot{\theta}_3 + h_5\dot{\theta}_2^2\sin(\theta_3 - \theta_2) + h_8\sin\theta_2$$

with

$$h_1 = J_1 + L_1^2(m_2 + m_3)$$
$$h_2 = L_1(m_2 l_2 + m_3 L_2)$$
$$h_3 = L_1 m_3 l_3$$
$$h_4 = J_2 + L_2^2 m_3 + l_2^2 m_2$$
$$h_5 = L_2 m_3 l_3$$
$$h_6 = J_3 + l_3^2 m_3$$
$$h_7 = \mathbf{g}(m_2 l_2 + m_3 L_2)$$
$$h_8 = \mathbf{g} m_3 l_3$$

Equation 4.15

If it is assumed that at the equilibrium point,

$$\theta_2 = \pi + \delta_2$$
$$\theta_3 = \pi + \delta_3$$
$$\dot{\theta}_2^2 = 0$$
$$\dot{\theta}_3^2 = 0$$
$$\sin\theta_2 = -\delta_2$$
$$\sin\theta_3 = -\delta_3$$
$$\cos\theta_2 = -1$$
$$\cos\theta_3 = -1$$
$$\cos(\theta_3 - \theta_2) = 1$$
$$\sin(\theta_3 - \theta_2) = \theta_3 - \theta_2$$

Then the equations of motion reduce to,

$$\tau - b_1\dot{\theta}_1 = h_1\ddot{\theta}_1 - h_2\ddot{\theta}_2 - h_3\ddot{\theta}_3$$
$$-b_2\dot{\theta}_2 = -h_2\ddot{\theta}_1 + h_4\ddot{\theta}_2 + h_5\ddot{\theta}_3 + h_7(\pi - \theta_2)$$
$$-b_3\dot{\theta}_3 = -h_3\ddot{\theta}_1 + h_5\ddot{\theta}_2 + h_6\ddot{\theta}_3 + h_8(\pi - \theta_3)$$

Equation 6.14

The linearised equations can then be written in matrix form as,

$$\begin{bmatrix} h_1 & -h_2 & -h_3 \\ -h_2 & h_4 & h_5 \\ -h_3 & h_5 & h_6 \end{bmatrix}\begin{bmatrix} \ddot{\theta}_1 \\ \ddot{\theta}_2 \\ \ddot{\theta}_3 \end{bmatrix} = \begin{bmatrix} \tau - b_1\dot{\theta}_1 \\ -h_7(\pi - \theta_2) - b_2\dot{\theta}_2 \\ -h_8(\pi - \theta_3) - b_3\dot{\theta}_3 \end{bmatrix}$$

$$Denote \begin{bmatrix} h_1 & -h_2 & -h_3 \\ -h_2 & h_4 & h_5 \\ -h_3 & h_5 & h_6 \end{bmatrix} by\ HH$$

Equation 6.15

To obtain the state space representation of the system the matrix multiplying the link accelerations was inverted and the equation multiplied by the result to get the expression in terms of the link accelerations independently. This was then rewritten in terms of the six states. The resulting equations are as follows in Equation 6.16.

$$\begin{bmatrix} \ddot{\theta}_1 \\ \ddot{\theta}_2 \\ \ddot{\theta}_3 \end{bmatrix} = HH^{-1} \begin{bmatrix} \tau - b_1\dot{\theta}_1 \\ -h_7(\pi - \theta_2) - b_2\dot{\theta}_2 \\ -h_8(\pi - \theta_3) - b_3\dot{\theta}_3 \end{bmatrix}$$

Now let

$$HH^{-1} = \begin{bmatrix} hh_1 & hh_2 & hh_3 \\ hh_2 & hh_4 & hh_5 \\ hh_3 & hh_5 & hh_6 \end{bmatrix}$$

And so the State Space representation is

$$\begin{bmatrix} \dot{\theta}_1 \\ \dot{\theta}_2 \\ \dot{\theta}_3 \\ \ddot{\theta}_1 \\ \ddot{\theta}_2 \\ \ddot{\theta}_3 \end{bmatrix} = \begin{bmatrix} 0 & 0 & 0 & 1 & 0 & 0 \\ 0 & 0 & 0 & 0 & 1 & 0 \\ 0 & 0 & 0 & 0 & 0 & 1 \\ 0 & hh_2h_7 & hh_3h_8 & -b_1hh_1 & -b_2hh_2 & -b_3hh_3 \\ 0 & hh_4h_7 & hh_5h_8 & -b_1hh_2 & -b_2hh_4 & -b_3hh_5 \\ 0 & hh_5h_7 & hh_6h_8 & -b_1hh_3 & -b_2hh_5 & -b_3hh_6 \end{bmatrix} \begin{bmatrix} \theta_1 \\ \theta_2 \\ \theta_3 \\ \dot{\theta}_1 \\ \dot{\theta}_2 \\ \dot{\theta}_3 \end{bmatrix} + \begin{bmatrix} 0 \\ 0 \\ 0 \\ hh_1 \\ hh_2 \\ hh_3 \end{bmatrix} \tau \quad \textit{Equation } 6.16$$

HH was defined parametrically and Matlab was used to invert the matrix. The state space representation is thus derived in the Matlab run script.

From the state space representation an LQR controller was designed using Matlab and implemented in Simulink.

6.2.3 Command Tracking Double Inverted Pendulum

A further point of interest for the inverted pendulum control was to have command tracking so that the horizontal link could be positioned anywhere between the physical bounds once the pendulum was in the inverted position. This was achieved by adding an offset to the measured angle of the horizontal link to make the LQR regulate about a different zero point.

7. CONTROL IMPLEMENTATION

Once the physical inverted pendulum system was constructed it was possible to test the control designs on the real rig. The progression of control that seemed logical to the authors was to start with stabilisation of the single inverted pendulum and then to implement swing up. Application of swing up and stabilisation control of the system would ensure global asymptotic stability of the upright equilibrium point. The final step would then be to implement stabilisation of the double inverted pendulum.

7.1 Experimental Topology

The first step in controlling the pendulum system was to interface it with the Personal Computer (PC) that would be used to test and develop the controller. The experimental rig was set up as shown in Figure 7.1.

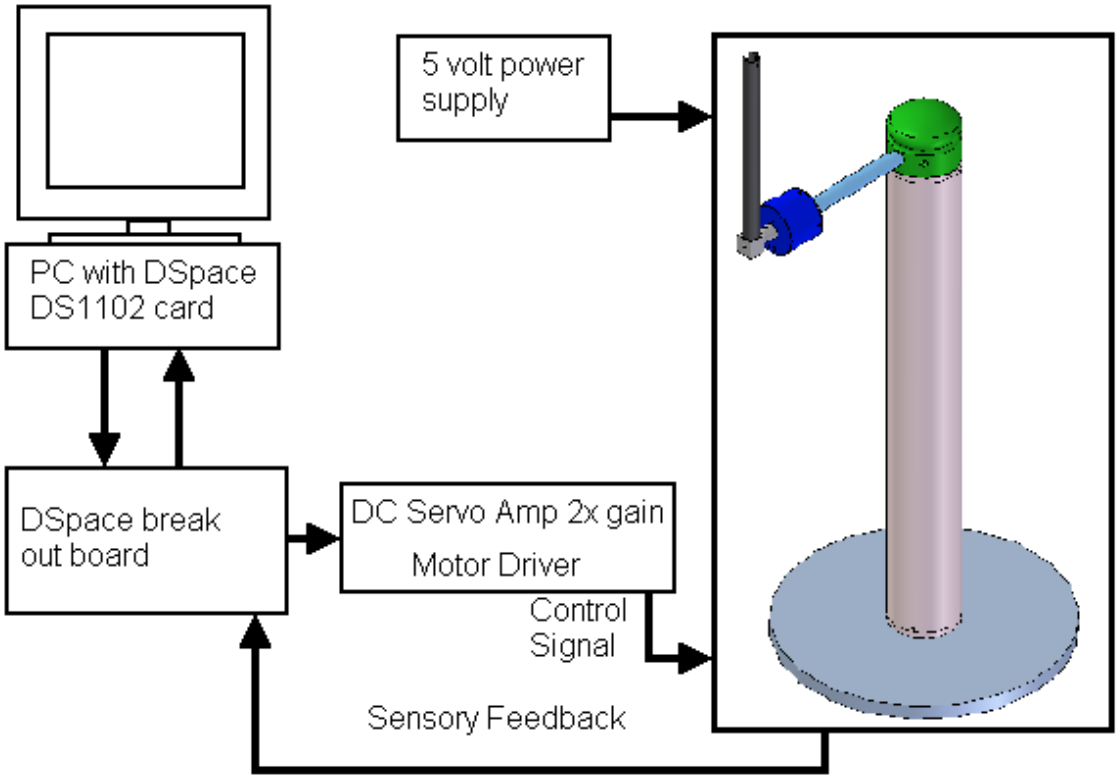

Figure7.1 Experimental layout of the inverted pendulum project shown in single pendulum mode.

As is shown in Figure 7.1 the first link in the control system is the PC fitted with the Dspace DS1102 card. The software applications running on the computer are Matlab / Simulink and Dspace control desk. With these systems in place, control development can be done rapidly with the system in operation. The second link in the control

system is the DSpace break out board. This allows the computer to be interfaced with sensory feedback and control output to the DC servo amplifier. The servo amplifier was used to supply the motor with the required voltage input and the additional power supply to power the sensory equipment.

With all the necessary connections between the equipment in place it was possible to calibrate the input / output connections so that the controller was seeing standard international units and the motor the desired supply voltage.

7.2 Stabilisation of the Single Inverted Pendulum

Having successfully set up the pendulum experimental rig it was possible to start implementing control. To stabilise the single inverted pendulum it was necessary to build a Simulink model incorporating the controller design to work with the DSpace card in the computer. The Simulink model is shown in Figure 7.2.

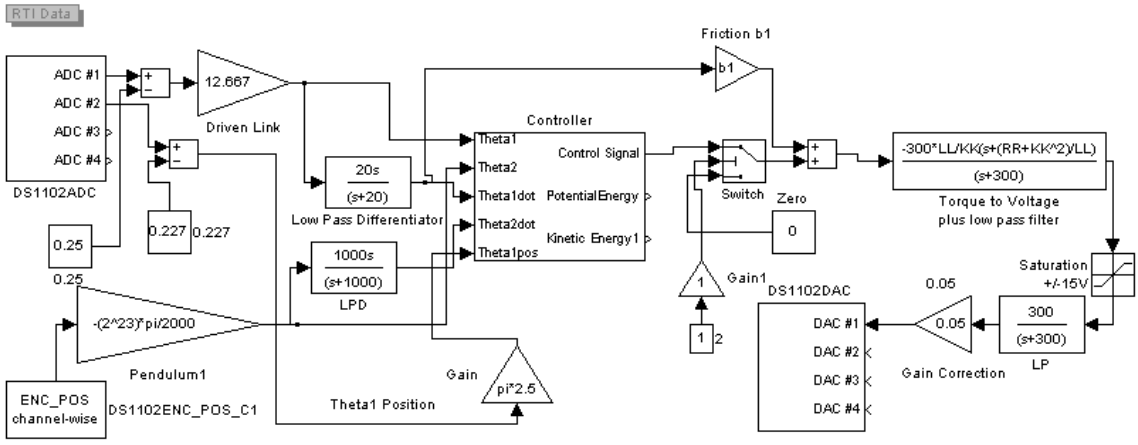

Figure7.2 Simulink model for experimental implementation, single pendulum.

The logic switch "Switch" in Figure 7.2 was added to allow the control to be switched on and off with the controller running. In Figure 7.2 it can be seen that calibration offsets and gains have been added to the controller to convert the raw data into the correct standard international units for the controller and the control output.

Running the controller as designed in virtual reality on the physical rig revealed that the data couple on the end of the horizontal link introduced significant levels of stiction (static friction). Manual tuning of the control gains improved the performance a little but the steady state response showed the existence of a limit cycle. This was overcome by adjusting the data couple until the carbon brushes no longer touched the power tracks (note that the second encoder is not attached in single pendulum mode).

With this done the controller was robust using the control developed on the modelled system. However it was noted that there was steady state error in the location of the horizontal link. To remove the steady state error an integral term was added to the error between horizontal (driven) link position and set point as shown in Figure 7.3. The integral term then drove the horizontal link to the desired set point. Integral gain was determined through manual tuning of the controller in virtual reality and then on the physical plant. This value of the integral gain is contained within the Matlab run script.

The controller as implemented with robust command tracking is shown in Figure 7.3.

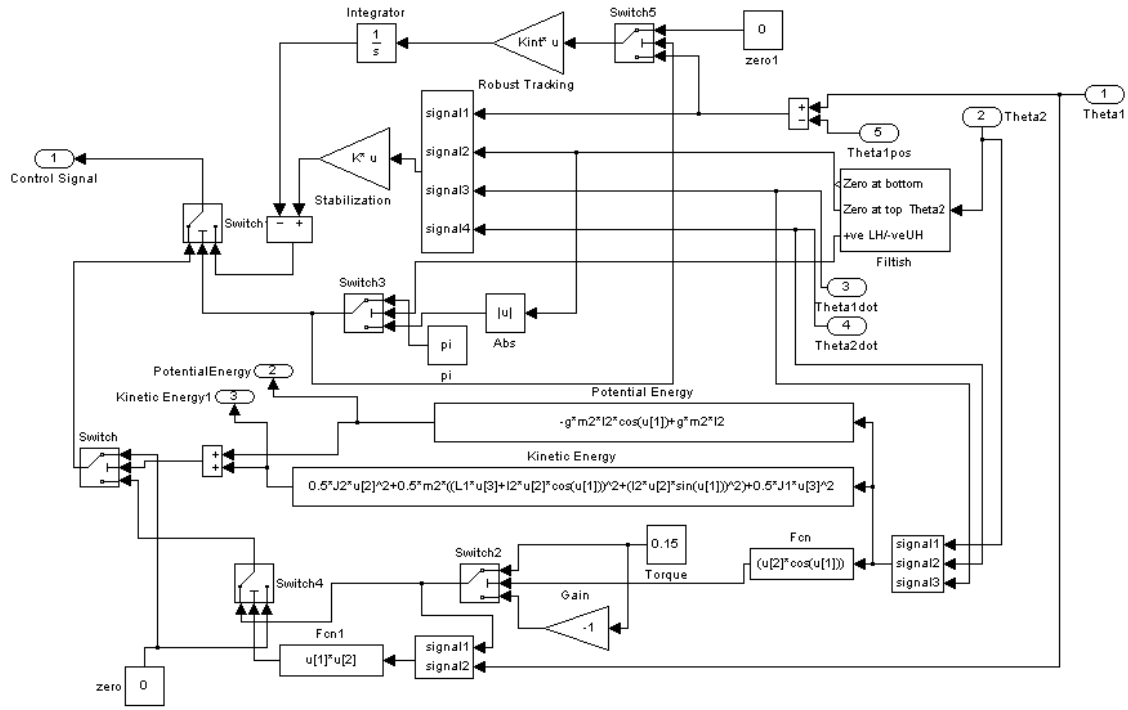

Figure7.3 The final control system for the single inverted pendulum.

7.3 Swing Up of the Single Inverted Pendulum

With balancing of the single inverted pendulum working only swing up would be required to achieve global asymptotic stability. During testing it was revealed that due to some modelling errors the cut off energy (the energy level at which the swing up controller stops inputting energy) was too low. Through manual tuning it was found that setting this threshold to between 0.6 and 0.7 the correct energy level could be achieved. One problem encountered was that with the power tracks of the data couple engaged the frictional dissipation of the system exceeded the maximum rate of energy

input and hence swing up could not be achieved. By disengaging the power tracks on the data couple and tuning the cut off energy swing up was achieved and hence global asymptotic stability. The swing up algorithm as implemented is shown in Figure 7.3.

7.4 Stabilisation of the Double Inverted Pendulum

Stabilisation of the double inverted pendulum is essentially the same as for the single inverted pendulum except that there is one more degree of freedom to sense and the modelling is a little more complicated. This said stabilisation of the double inverted pendulum was not achieved in reality. As mentioned in section 7.2 Stabilisation of the Single Inverted Pendulum the data couple introduced significant stiction to its rotary joint. In addition to this problem the power transfer across the data couple was unreliable and the data itself was susceptible to corruption due to ambient light and bleeding between the two optical tracks. Due to these issues no testing was undertaken as there was a low probability of achieving any reasonable performance.

Although no actual testing of the double inverted pendulum could be undertaken some control design improvements could be made based on the results of the single inverted pendulum. Namely it was deduced that an integral term would need to be added to achieve robust command tracking in the double inverted pendulum. The resulting Simulink model used to interface with DSpace and the finalised controller are shown in Figure 7.4 and Figure 7.5. Note the inclusion of calibration gains and offsets.

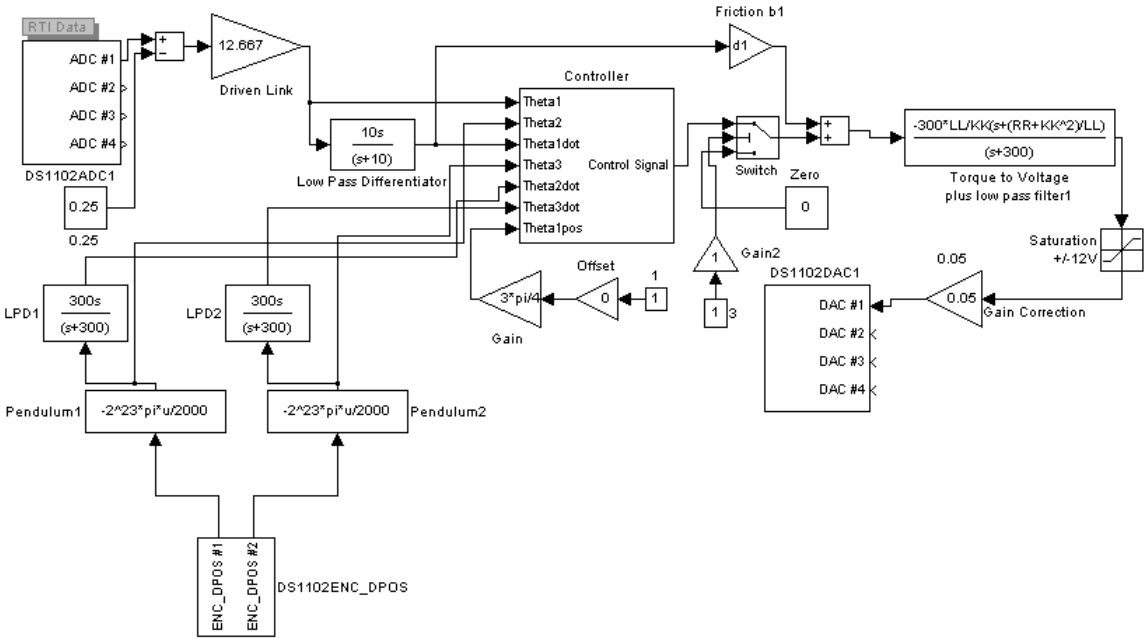

Figure7.4 Simulink model for experimental implementation, double pendulum.

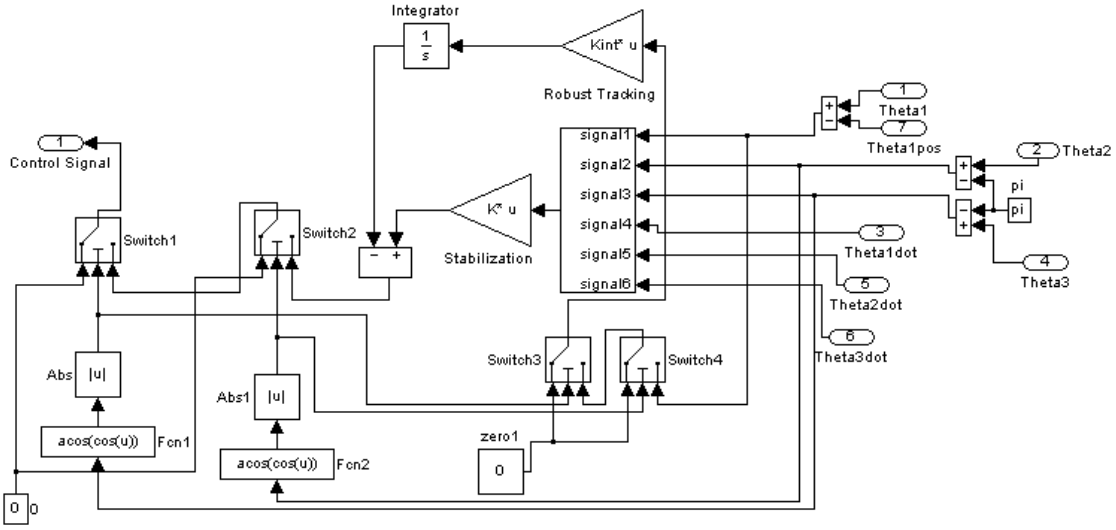

Figure7.5 The final control system for the double inverted pendulum.

8. RESULTS

The inverted pendulum project has resulted in various levels of success.

Global asymptotic stability (GAS) of the single inverted pendulum was achieved in real time on the physical system with good repeatability and good robustness. (See Figure 8.1.)

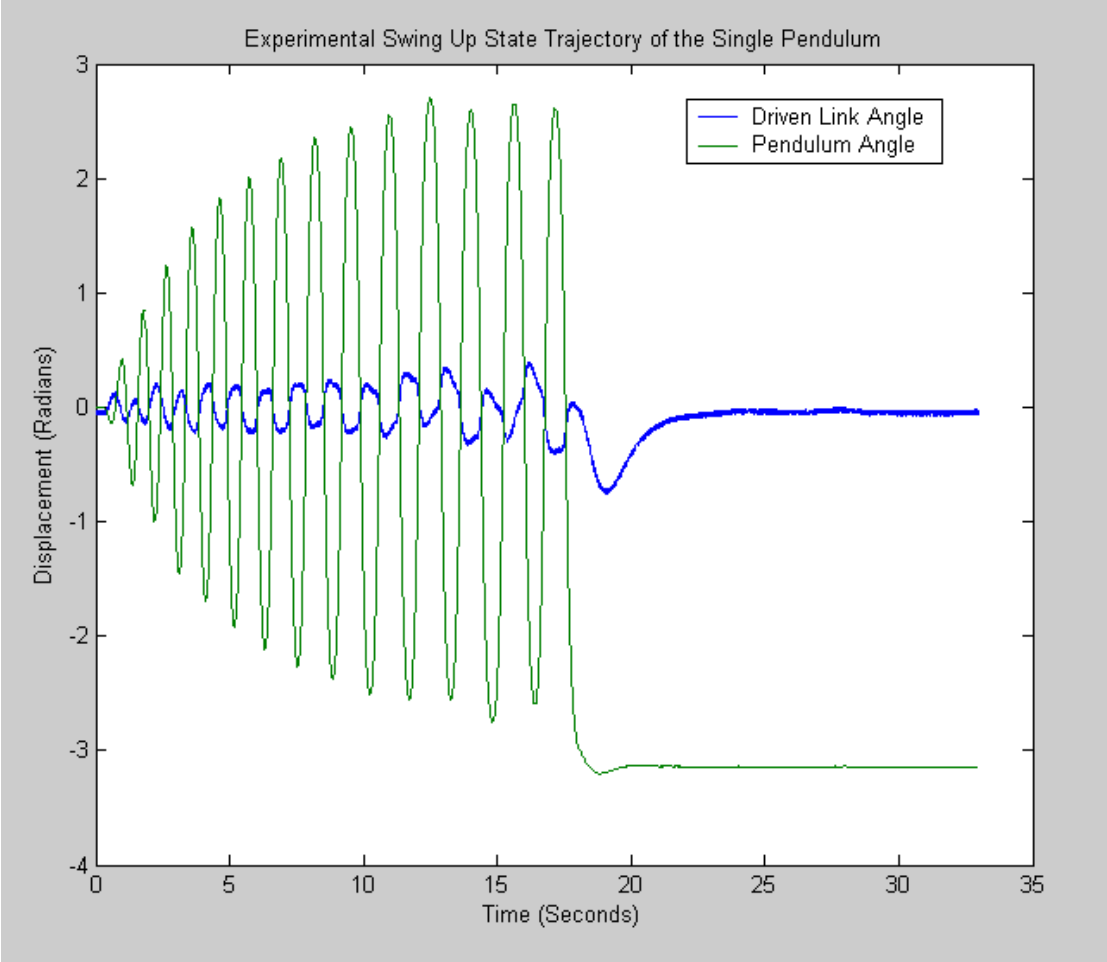

Figure 8.1 Experimental swing up of the single pendulum.

From the results shown in Figure 8.1 it can be seen that the maximum rate of energy input is close to rate of energy being lost from the system, evident from the logarithmic envelope about the pendulum displacement. In simulation better results have been achieved using larger control torques in the same swing up algorithm, hence to improve swing up performance the system mass needs to be reduced and therefore the effective control torque increased. Results from simulation with a control torque of 0.25 Nm are shown in Figure 8.2.

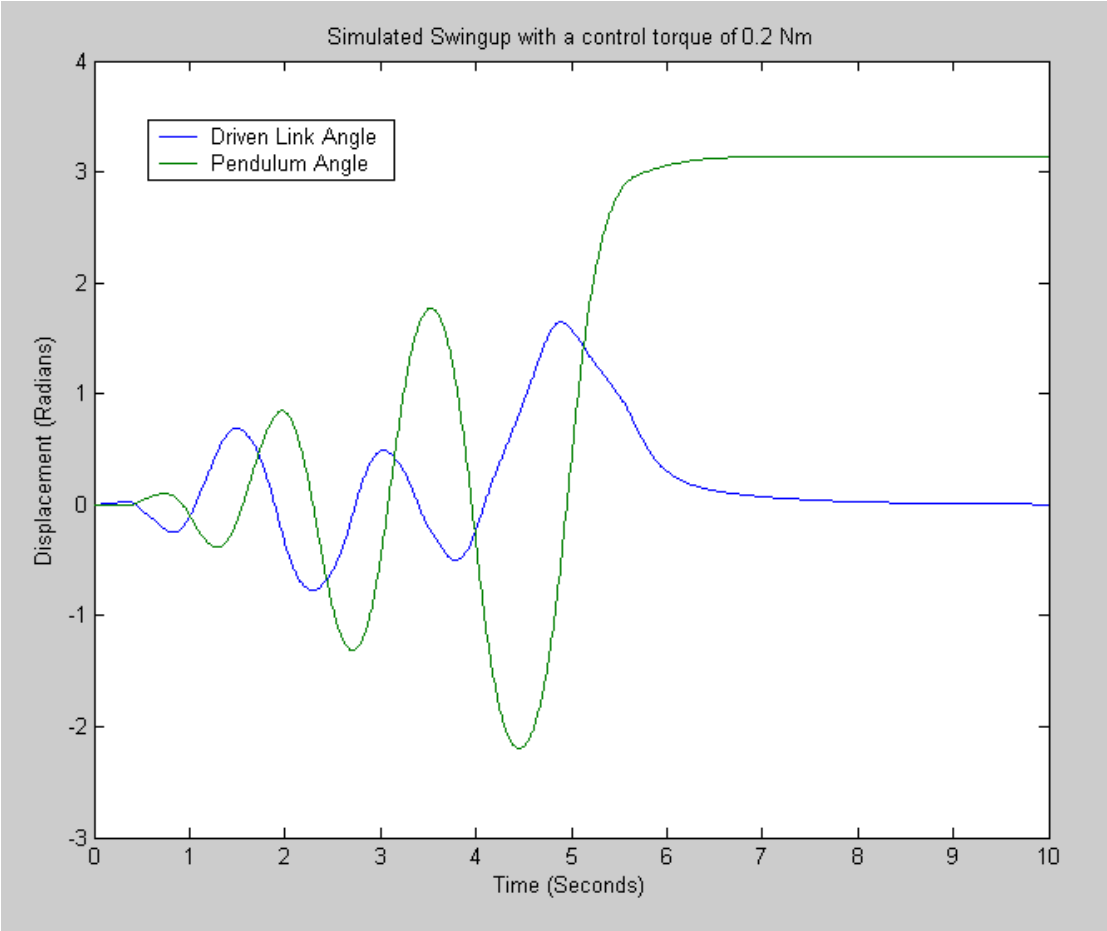

Figure 8.2 Simulated swing up with a control torque of 0.25 Nm.

Reliable command tracking has also been achieved in real time as is shown in Figure 8.3. It can be seen in Figure 8.3 that there is a small level of deviation from the set point in the settled system.

The steady state response of the controlled single inverted pendulum system revealed large amounts of noise in the control signal. This noise is the probable cause of the deviation seen in the links from the settled positions. It was determined that the source of this noise was the differentiation of the encoder output. At low velocity the differentiated encoder signal produces large spikes when the encoder clicks over a pulse. This velocity is then multiplied by a gain, clipped by a saturation block set and fed back, hence the excessive level of noise in the control signal. This was overcome by adding a low pass filter after the saturation block. This greatly reduced the audible noise generated by the plant. However large control signals due to the differentiation noise of the encoder were still present. To overcome this problem some other method of velocity estimation needs to be assessed and finally implemented in future work. The steady state control signal is shown in Figure 8.4.

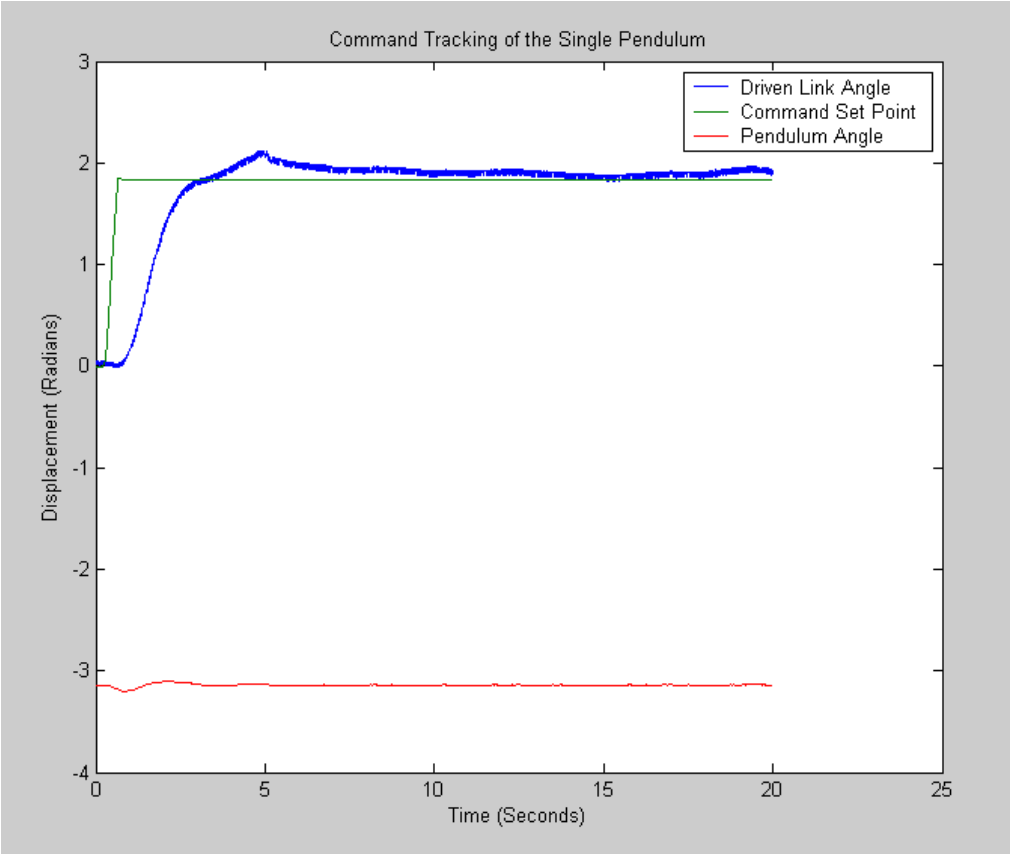

Figure 8.3 Experimental step response of the single pendulum.

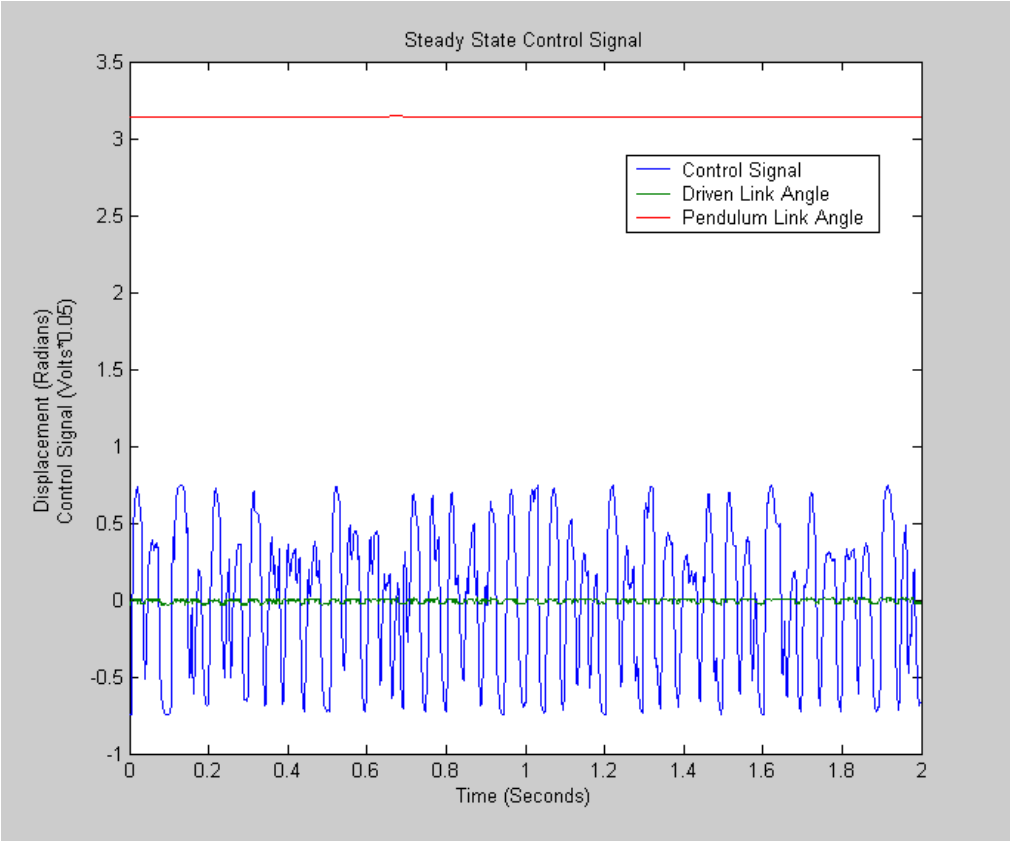

Figure 8.4 Steady state control signal.

Having successfully controlled the single inverted pendulum it was time to implement control on the double inverted pendulum. However whilst the rig was being operated in single pendulum mode it was noticed that the LED's on the data couple were flashing (with the data couple engaged) whereas they should have been permanently on. This indicates that the power supply to the LED's was unreliable even without the added load of the encoder on the power supply. Hence it was not justified to expect the reliable data transfer required to execute control.

Another point of concern was the excessive mass of the system. It was feared that with the large mass of the encoder housing if the controller went unstable and the pendulum links fell the encoder or the motor would be damaged. Further the experimental rig has appeared to have low stiffness in the horizontal link. It was later determined that this was due to the lack of a second grub screw fastening the manual input knob to the motor shaft and hence allowing the horizontal to pivot elastically on the single grub screw.

9. EXHIBITION

An important part of final year projects is the project exhibition. The inverted pendulum was on display, and it was definitely a crowd favourite. The single inverted pendulum ran all day, showing swing-up control, stabilisation control, and command tracking. Since the pendulum was built as a demonstration tool, able to withstand manual disturbances and attempts at manual control, people were invited to play with the pendulum. Some people returned several times to show their friends and family how the pendulum worked.

Command tracking was demonstrated using a computer games' steering wheel. The controller made the horizontal link follow the angular position of the steering wheel. A similar interactive quality was brought to the double inverted pendulum using a joystick for command input.

The inverted pendulum was very successful as a control demonstration. Undergraduate students studying automatic control subjects had lots of questions about the pendulum and controller. Having the pendulum in operation, with controller block diagrams on display was a great way to answer their questions. The Authors spent lots of time talking interested parties through the design process, which also added to their understanding of the project and the engineering process in general.

The Project exhibition was a sponsored event, and prizes were awarded at the end of the day. Projects were assessed by a panel of judges, made up of industry sponsors and academics. The inverted pendulum project was awarded the Schefanacker Award for best overall project. For this the Authors give thanks to the workshop staff, supervisors, friends and family for their support and help throughout the project.

10. COSTING

Engineering work is never undertaken in its own right. Design exists in an environment of market requirement and economic viability. The introduction and project specification set out that there was a market for this project to be conducted. Section 10 reviews the financial cost of developing the double inverted pendulum.

10.1 Current Cost

Commercial inverted pendulum experimentation rigs are commercially available from Quanser and Googol Technologies. One of the aims of the project was to produce the pendulum system at lower cost than buying a control experiment. Table 10.1 gives a summary of the costs incurred in developing the pendulum system.

Table 10.1 Project expenditure

Item	Quantity	Cost/Unit	Cost
Real Costs			
Servo Motor	1	262.00	$ 262.00
Encoder	2	341.00	$ 682.00
Potentiometer	1	95.60	$ 95.60
Materials - Electronic Workshop	1	41.82	$ 41.82
Materials - Mechanical Workshop	1	89.55	$ 89.55
Workshop Time - Electronic (hrs)	70	35.00	$ 2,450.00
Workshop Time - Mechanical (hrs)	68	35.00	$ 2,380.00
Total Real Cost			$ 6,000.97
Virtual Costs			
Researcher time (hrs)	623	26.00	$ 16,198.00
Direct Costs	623	7.80	$ 4,859.40
Indirect Costs	623	33.80	$ 21,057.40
Total Virtual Cost			$ 42,114.80
Total			$ 48,115.77

Table 10.1 is divided into real and virtual costs. The real costs include components, materials and the labour cost for workshop staff. The virtual cost is how much the project would have cost if the researchers were being paid for their time. The virtual calculations are based on an hourly rate of $26 per researcher, an extra 30% to cover superannuation, payroll tax, workcover, long service and leave that would be directly associated with the labor cost of this project, and an extra 130% for administration, technical support, infrastructure, rent, telephone and internet, that would be shared

costs between all work being undertaken. So in real cost incurred, the inverted pendulum system has cost the School of Mechanical Engineering $6000. Commercial systems sell for between $5000 and $11600, (see appendix D), the cheaper systems having fewer degrees of freedom. At $6000, the double inverted pendulum has been delivered at a competitive price.

Had the project been run in a research and development company, where the researchers were paid, the project would have cost over $50,000. Keeping track of the time invested in this project, and giving it a monetary value shows that engineering design effort is an expensive commodity. It also suggests that if the research and development company wanted an inverted pendulum rig for control experimentation, it would have been cheaper to buy one off the shelf.

10.2 Future Cost

It has been suggested by the project supervisors, and the authors agree that further development of the double inverted pendulum system should be investigated. Section 11 outlines the work that should be undertaken, while a brief analysis of the cost of extending this project is presented here. Table 10.2 shows the areas in which the project is foreseen to develop, and gives an estimation of the costs involved in pursuing the design goals.

Table 10.2 Future project costs

Design Goal	Associated requirement	Cost estimate
Reduce System Mass		
	New materials	$ 100.00
	Smaller encoders	$ 800.00
	Workshop time	$ 2,000.00
Increase Control Torque		
	Motor	$ 500.00
Improve Data Couple		
	New electronics	$ 100.00
	Workshop time	$ 2,000.00
Stand Alone Operation		
	Micro-controller	$ 300.00
	RS-232 converter for encoders	$ 200.00
	Servo Amplifier	$ 100.00
Total		$ 6,100.00

11. FUTURE WORK

As a poem is to a poet or a song is to a songwriter, is a project to an engineer, the question may be posed as to whether there is ever a point at which one can say that it is finished. With this in mind there is always a point at which work ceases, whether induced by deadlines, death or otherwise.

With the prospect that work on this particular project is likely to continue in the future it seems fitting to show those taking on the task, the direction of the departing participants.

The project, “Design, build and control a double inverted pendulum”, has resulted in the creation of a grand starting point for coming years. As is described in the preceding text a working single inverted pendulum with global asymptotic stability of the unstable upright equilibrium position has been achieved. In simulation stabilisation of a double inverted pendulum system has also been achieved. However impressive these feats in control application and system construction are, there are some shortcomings to be addressed. Analytic scrutiny of the project outcomes begins with a look at the mechatronic design and will proceed into the controller design. It should be noted at this point that system and controller design are coupled and should work together to produce the best possible system performance.

11.1 Future Mechatronic System Development

Continuing improvement of the mechatronic design will see a number of pertinent issues addressed. The first and most important shortcoming of the existing mechatronic design is the mass of the system. Due to the large size of the encoders and encoder housings the horizontal and first pendulum links in the double pendulum configuration are excessively massive. This was a result of trying to achieve good aesthetic qualities and to incorporate high precision encoders with enough structural integrity to support the pendulum links. At the time of selection of the encoders it was desired to have approximately 1000 encoder pulses per revolution to yield approximately 1000 measurement points per revolution. However it was not realised that DSpace and the encoders read in quadrature meaning that there are four measurements per encoder pulse. This means that the chosen encoders have approximately four times the required precision required. An alternative design may utilise smaller encoders that may fit within the pendulum tubes. The pendulum links

may then be supported with some kind of bearing-shaft arrangement substantially reducing the mass of the pendulum links.

An alternative to reducing the mass is to increase the torque available from the motor. Testing showed that the controller was attempting to drive the motor with 40 volt impulses. This would have been quite detrimental, so the output voltage was limited to 15 volts. Having a larger motor, capable of handling higher voltage would make swingup quicker and balancing more stable.

In order to achieve control of the double inverted pendulum system a reliable data transfer system is needed to transfer data from the encoder on the end of the first pendulum link. The existing design was developed from the conceptual ideas that appeared most feasible. An improved design would address the unreliable power supply to the encoder side of the data link and improve frequency response of the data transfer by isolating the optical data transfer from extraneous noise sources.

The pendulum system is currently tethered to a personal computer. It would be a more convenient demonstration tool if it could stand alone from other bulky pieces of equipment. To achieve this, a micro-controller could be used, and hidden to preserve the neat exterior of the pendulum system.

Control of a triple inverted pendulum is not infeasible, and even four links balanced serially has been seen in video footage over the internet (Googol Technology, 2004). Once balance of the double inverted pendulum was achieved, future designers could extend the system to more links.

11.2 Future Control System Development

The final controllers developed for both the single and double inverted pendulum systems have obtained adequate performance within the bounds of the author's abilities to test them. The upright regulator for the double inverted pendulum as implemented in simulation shows reasonable command point tracking and robustness. The fact that the data couple for the second encoder failed to operate successfully and the questionable structural integrity of the double inverted pendulum make real system testing unfeasible for this year's project.

Control of the single inverted pendulum achieved global asymptotic stability with good disturbance rejection on the physical system. However under operating conditions there is a large quantity of noise in the control input at static equilibrium.

The source of this large noise is the derivative term on the encoder telling the controller the velocity of the pendulum link. Overcoming the excessive noise would involve either implementing an observer or some kind of Kalman Filter to compensate for the noise in the velocity measurement. Future work should include research into methods of reducing the noise in the velocity estimate. A good start would be the paper entitled An Adaptive Kalman Filter with Quadrature Encoder Quantisation Compensation, (Katupitiya and Luong, circa 2001).

Finally swing up of the double inverted pendulum should be pursued. Two papers which may be a good start are Swinging-up and Balancing Control of Double Fututa Pendulum by Using State-Dependent Riccati Equation (Kobayashi et. al., circa 2001), Rotational Control of Double Pendulum (Komine et. al., circa 2000)

12. CONCLUSION

Overall, the project "Design, build and control a double inverted pendulum" has been very successful. A modular double inverted system has been designed and built within one academic year. Control algorithms have been investigated, written and proven in the real world for the single inverted pendulum. Swing-up control of the single inverted pendulum was also achieved. A mathematical model of the double inverted pendulum has been developed, and this has lead to the development of a double inverted pendulum balancing controller. The double pendulum controller has been seen to work in virtual reality.

The main goal of this project was to produce an experimental device that could showcase modern control, and be used in undergraduate lectures or laboratories as well as departmental exhibitions. Even before this project was completed, undergraduate students were being told to see the inverted pendulum exhibition (Yong K. Lee, 2004). The authors are proud to say that they were not disappointed.

There is still scope for further development, as continuation of this project would see refining the mechatronic design, addressing the control noise associated with the velocity feedback and swinging up the double inverted pendulum. Further development will see additional pendulum links added to the mathematical models and or the physical system.

REFERENCES

Åström, K. J. and Furuta, K. (1996). Swinging up a Pendulum by Energy Control, *Paper presented at IFAC 13th World Congress, San Francisco, California, 1996.*

Brokett, R.W. and Hongyi LI. (2003). A Light Weight Double Pendulum: Maximising The Domain Of Attraction, *Proceedings of the IEEE Conference on Decision and Control*, v 4, 2003, p 3299-3304

Cazzolato, B. Ph.D

a group meeting 16/03/2004

b advanced automatic Control lecture 18/05/2004

Department Of Mechanical Engineering, at The California Institute Of Technology (1994). Analysis And Control Of An Inverted Pendulum. *Laboratory hand out.*

Dorf, R.C. and Bishop, R.H. (1998). *Modern Control Systems 8th edition,* Addison Wesley Longman: California USA.

Efunda, (2004) World Wide Web link, www.efunda.com/ accessed (30/08/2004)

Fossard, A.J. and Normand-Cyrot, D. (1997). *Nonlinear Systems Volume 3 Control,* London: Chapman & Hall.

Franklin, G.F., Powell, J.D., Emami-Naeini, A. (2002). *Feedback Control Of Dynamic Systems ,* New Jersey: Prentice Hall.

Googol Technology Ltd., 2004. World Wide Web link

www.googoltech.com.cn accessed (2/8/2004)

Katupitiya, Van Jayantha and Luong Daniel (circa 2001). An Adaptive Kalman Filter with Quadrature Encoder Quantisation Compensation, *School of Mechanical and Manufacturing Engineering University of New South Wales Sydney, Australia.*

Kobayashi, Iwase, Suzuki, Furuta (circa 2001). Swinging-up and Balancing Control of Double Fututa Pendulum by Using State-Dependent Riccati Equation, *Graduate School of Systems Engineering, Tokyo Denki University.*

Komine, Iwase, Suzuki, Furuta (circa 2000). Rotational Control of Double Pendulum, *Graduate School of Systems Engineering, Tokyo Denki University Hatoyama-cho, Hiki-gun, Saitama, Japan.*

Mathworks, (2004) World Wide Web link, www.mathworks.com/ accessed (15/4/2004)

Max Plank Institute, (2004). World Wide Web link wwwa.mpi-magdeburg.mpg.de/research/pendel/index_e.html accessed (12/4/2004)

Quanser Consulting Inc (2004), www.quanser.com accessed (10/05/2004)

Rubi, J. and Avello A. (2002). Swing Up Control Problem For a Self Erecting Double Inverted Pendulum, *IEE Proceedings Of Control Theory Application,* v 149, No.2 March 2002

Rubi, J. and Avello A. (2002). World Wide Web link http://www.tecnun.com/asignaturas/Controll/Proyectos/pdobleinv/evideo.htm (10/04/04)

Utkin, V., Gulder, J., SHI, J. (1999). *Sliding Mode Control In Electromechanical Systems,* Pudstow:T.J. International Ltd.

Wolfman, (2004) World Wide Web link, http://wolfman.eos.uoguelph.ca/~jzelek/matlab/ctms/examples/motor/motor.htm accessed 6/10/2004

Wolfram Research, (2004) World Wide Web link, http://mathworld.wolfram.com/TaylorSeries.html accessed 19/10/2004

Yong. K. Lee, 2004.
E-mail to undergraduate students. 16/8/2004

Zander, A, 2004, Vibrations 3012, Undergraduate course notes, School of Mechanical Engineering, The University of Adelaide.

Zhong, W. and Röck, H.. (2001). Energy And Passivity Based Control Of The Double Inverted Pendulum On Cart, *2001 IEEE Conference On Control Applications,* p 896-901

APPENDIX A

The Matlab scripts for the single and double inverted pendulum systems.

Single inverted pendulum,

```
clc;
clear all;
close all;

%Here we have the model of a single rotary inverted pendulum system
m2=0.075*1;    %mass of the pendulum kg  + fudge factor
b1=0.0001;  %friction of the motor rotor Nmsec
b2=0.00028;  %friction of the pendulum  Nmsec
l2=0.148*1;    %length to pendulum center of mass m  + fudge factor
%l2=0.269;    %length to pendulum center of mass m with encoder on end
L1=0.278;   %length of rotor rod m
J1=2.27*10^(-2);  %inertia of the rotor kg*m^2
J2=3.86*10^(-3);  %inertia of the pendulum kg*m^2
%J2=3.04*10^(-2);  %inertia of the pendulum kg*m^2 with encoder on end
g=9.8;     %Acceleration due to gravity m/s^2
wo=sqrt(m2*l2*g/J2);%Natural frequency for small pertubations about stable equilibria
%Motor properties
KK=0.09;    %N/amp
LL=0.005;   %H
RR=7.8;     %Ohms

%Now we want to define the state space equation linearized about theta2=pi
h1=m2*l2^2+J2;
h2=m2*l2*L1;
h3=(J1+m2*L1^2);
```

```
h4=m2*l2*L1;
P=((J1+m2*L1^2)*(J2+m2*l2^2)-m2^2*l2^2*L1^2);

%The A matrix is:
A=[0,0,1,0;0,0,0,1;0,m2*l2*h4*g/P,-b1*h1/P,-b2*h2/P;0,h3*m2*l2*g/P,-b1*h4/P,-
b2*h3/P];
%The b matrix is:
b=[0;0;(m2*l2^2+J2)/P;m2*l2*L1/P];
c=[1,1,1,1];
d=[0];
penny=ss(A,b,c,d);
disp('The open loop poles are:')
pole(penny)
disp('The open loop zeros are:')
zero(penny)

%Try an LQR design
N=zeros(4,1);
Q=[1,0,0,0;0,0.1,0,0;0,0,1,0;0,0,0,1];
R=[10];
[K,S,E] = LQR(A,b,Q,R,N);
penny_ppL = SS(A-b*K,b,c,d);
disp('The closed Loop poles for the LQR are:')
disp(pole(penny_ppL))

%Integral Gain
Kint=0.02;
```

```
Double inverted pendulum,
clc;
close all;
clear all;

%Script for double inverted pendulum model SI units
L1=0.278;   %Length of horizontal link
L2=0.313;    %Length of middle link
l2=0.269;    %distance from horizontal link to centre of gravity of
        %middle link
l3=0.152;    %distance from end of middle link to centre of gravity of
        %end link
m2=0.37;    %mass of link 2
m3=0.088;    %mass of link 3
J1=2.48*10^(-2); %Inertia of link 1 about it's centre of rotation
J2=3.04*10^(-2); %Inertia of link 2 about it's centre of gravity
J3=5.61*10^(-3); %Inertia of link 3 about it's centre of gravity
d1=0.0001;  %damping in motor bearings
d2=0.00028;  %damping in encoder1 bearings
d3=0.00028;  %damping in encoder2 bearings
g=9.81;    %Acceleration due to gravity
wo=sqrt((m2+m3)*g*((l2+L2+l3)/2)/(J2+J3+l2^2*m2+(L2+l3)^2*m3));
%Motor properties
KK=0.09;    %N/amp
LL=0.005;   %H
RR=7.8;     %Ohms

H1=J1+(m2+m3)*L1^2;
H2=L1*(m2*l2+m3*L2);
```

```
H3=m3*L1*l3;
H4=J2+m2*l2^2+m3*L2^2;
H5=m3*l3*L2;
H6=J3+m3*l3^2;
H7=g*(m2*l2+m3*L2);
H8=m3*l3*g;

%Define the state equation
A=zeros(6,6);
sv=[H1 -H2 -H3;-H2 H4 H5;-H3 H5 H6];
sinv=inv(sv);

for i=1:3
   A(i,i+3)=1;
end
A(4,2)=sinv(1,2)*H7;
A(5,2)=sinv(2,2)*H7;
A(6,2)=sinv(3,2)*H7;
A(4,3)=H8*sinv(1,3);
A(5,3)=H8*sinv(2,3);
A(6,3)=H8*sinv(3,3);
A(4,4)=-d1*sinv(1,1);
A(5,4)=-d1*sinv(2,1);
A(6,4)=-d1*sinv(3,1);
A(4,5)=-d2*sinv(1,2);
A(5,5)=-d2*sinv(2,2);
A(6,5)=-d2*sinv(3,2);
A(4,6)=-d3*sinv(1,3);
A(5,6)=-d3*sinv(2,3);
```

```
A(6,6)=-d3*sinv(3,3);

b=[0;0;0;sinv(1,1);sinv(2,1);sinv(3,1)];
c=[1 1 1 1 1 1];
d=[0];

penny=ss(A,b,c,d);
disp('The open loop poles are:')
pole(penny)
disp('The open loop zeros are:')
zero(penny)

%Try an LQR design
N=zeros(6,1);
Q=[1,0,0,0,0,0;0,1,0,0,0,0;0,0,1,0,0,0;0,0,0,1,0,0;0,0,0,0,1,0;0,0,0,0,0,1];
R=[10];
[K,S,E] = LQR(A,b,Q,R,N)

k1=K(1,1);
k2=K(1,2);
k3=K(1,3);
k4=K(1,4);
k5=K(1,5);
k6=K(1,6);
penny_ppL = SS(A-b*K,b,c,d);

disp('The closed Loop poles for the LQR are:')
disp(pole(penny_ppL))
Kint=0.01;
```

APPENDIX B

Taylor Series expansion for a multivariable equation

$$f(x_1,\ldots,x_n)=\sum_{j=0}^{\infty}\left\{\frac{1}{j!}\left[\sum_{k=1}^{n}(x_k-a_k)\frac{\partial}{\partial x_k'}\right]^j f(x_1',\ldots,x_n')\right\}_{x_1'=a_1,\ldots,x_n'=a_n}.$$

(Wolfram Research, 2004)

APPENDIX C

----- Forwarded message from yong.k.lee@adelaide.edu.au -----

Date: Sat, 16 Oct 2004 01:40:07 +0930 (CST)

From: yong.k.lee@adelaide.edu.au

Reply-To: yong.k.lee@adelaide.edu.au

Subject: Good Luck in your studies!

To: yong.k.lee@adelaide.edu.au

Yo!

A BIG thanks to those who co-operated and worked along with me in the last 3 pracs without which we wouldn't be able to finish 2 exercises in 3 hours :D

I hope that everyone have learnt something and enjoyed the Automatic Control Prac very much!

Don't worry too much about your report write-up.
Don't waste too much time on it. Pay more attention to your coming exams. If you followed what i have told you - answer all the questions and summarize what

you have learnt, you are likely to be a WINNER.

We guarantee that you will NOT get 0/10 unless you did not submit a report OR you did not attend the prac OR you copied someone else report. No one will get 0/10 without any reason. If you attended the prac and have submitted a report, then you shouldn't need to worry at all. We are very understanding people.
Don't worry and take it easy!

One more thing worth mentioning:
There is a Final Year Project exibition on friday 22 Oct 2004. I strongly recommend you to attend. Pay attention to the "Inverted Pendulum"'s project.. and u will get a better understanding of AUTOMATIC CONTROL subject and it's real POWER and Application!!!

Wish you all the best in your studies
and hope you'll get flying colours results in your final exams!
Good Luck!

Best wishes from
Yong-Keat (i am NOT "Yong" BUT "Yong-Keat")
Automatic Control Prac Tutor/Demonstrator

----- End forwarded message -----

APPENDIX D

Hi James,

Thank you very much for your inquiry.

There are so many inverted pendulum configurations.

Linear, Plainer and Circular.

Within Linear, there are 4 models. single stage up to 4 stages.

Could you tell me which ones you are interested in?
The price range is from US$3,600 up to US$8,400.

Please let me know.

Thank you very much.

Eimei Onaga
_/
Eimei Onaga
President, Innovation Matrix, Inc.
+1 408-329-4422 (TEL)
+1 650-714-6398 (Mobile)
+1 408-716-2553 (FAX)
eonaga@innovation-matrix.com
www.innovation-matrix.com
_/

-----Original Message-----
From: info@innovation-matrix.com [mailto:info@innovation-matrix.com]
Sent: Monday, October 18, 2004 4:29 PM
To: info@innovation-matrix.com
Subject: Feedback: from innovation-matrix.com

First Name: James

Last Name: Driver

Title:

Company Name: The University of Adelaide

Address: North Terrace

City: Adelaide

State:

State/Provice (Out side USA): Fill out if you are outside USA

Country: Australia

Zip Code:

Email: james.driver@student.adelaide.edu.au

Home Phone:

Work Phone:

Cellphone:

Fax:

Inquiry: Hello,

I'm doing my honours engineering studies in automatic control and I'm interested in the list price of the googol inverted pendulum experiments. Your help is greatly appreciated.

Thankyou,

James

Machine Vision Components: No

Inspeciotn Software: No

Motion Control Cards: No

Intelligent Touch Monitor: No

Systems and Solutions: No

Robots: No

Send Company Literature: No

Have a salesperson contact me: No